Protein Zero, a Nervous System Adhesion Molecule, Triggers Epithelial Reversion in Host Carcinoma Cells

Joseph P. Doyle,[‡] Jerome G. Stempak,[‖] Pamela Cowin,[¶] David R. Colman,[*] and Donatella D'Urso[§]

*The Brookdale Center for Molecular Biology, The Mount Sinai School of Medicine, New York 10029;[‡]Center for Neurobiology and Behavior, College of Physicians and Surgeons, Columbia University, New York 10032;[§]Neurologische Klinic, Neurochemisches Lab., University of Düsseldorf, 40225 Düsseldorf;[‖]Department of Anatomy and Cell Biology, Health Science Center, Brooklyn, New York 11203; and [¶]Departments of Cell Biology and Dermatology, New York University School of Medicine, New York, New York 10016

Abstract. Protein zero (P_0) is the immunoglobulin gene superfamily glycoprotein that mediates the self-adhesion of the Schwann cell plasma membrane that yields compact myelin. HeLa is a poorly differentiated carcinoma cell line that has lost characteristic morphological features of the cervical epithelium from which it originated. Normally, HeLa cells are not self-adherent. However, when P_0 is artificially expressed in this line, cells rapidly aggregate, and P_0 concentrates specifically at cell–cell contact sites. Rows of desmosomes are generated at these interfaces, the plasma membrane localization of cingulin and ZO-1, proteins that have been shown to be associated with tight junctions, is substantially increased, and cytokeratins coalesce into a cohesive intracellular network. Immunofluorescence patterns for the adherens junction proteins N-cadherin, α-catenin, and vinculin, and the desmosomal polypeptides desmoplakin, desmocollin, and desmoglein, are also markedly enhanced at the cell surface. Our data demonstrate that obligatory cell–cell adhesion, which in this case is initially brought about by the homophilic association of P_0 molecules across the intercellular cleft, triggers pronounced augmentation of the normally sluggish or sub-basal cell adhesion program in HeLa cells, culminating in suppression of the transformed state and reversion of the monolayer to an epithelioid phenotype. Furthermore, this response is apparently accompanied by an increase in mRNA and protein levels for desmoplakin and N-cadherin which are normally associated with epithelial junctions. Our conclusions are supported by analyses of ten proteins we examined immunochemically (P_0, cingulin, ZO-1, desmoplakin, desmoglein, desmocollin, N-cadherin, α-catenin, vinculin, and cytokeratin-18), and by quantitative polymerase chain reactions to measure relative amounts of desmoplakin and N-cadherin mRNAs.

P_0 has no known signaling properties; the dramatic phenotypic changes we observed are highly likely to have developed in direct response to P_0-induced cell adhesion. More generally, the ability of this "foreign" membrane adhesion protein to stimulate desmosome and adherens junction formation by augmenting well-studied cadherin-based adhesion mechanisms raises the possibility that perhaps any bona fide cell adhesion molecule, when functionally expressed, can engage common intracellular pathways and trigger reversion of a carcinoma to an epithelial-like phenotype.

Cell–cell contact in a forming epithelial monolayer is believed to be initiated by cell adhesion molecules (CAMs)[1] that are Ca^{++} dependent, as exemplified by E-cadherin (Gumbiner et al., 1988; Takeichi, 1991; Wollner et al., 1992). This contact is maintained and reinforced by the generation of characteristic junctional complexes composed mainly of tight junctions, subjacent adherens junctions, and desmosomes (Farquhar and Palade, 1963; and see Rodriguez-Boulan and Nelson, 1989). The tight junctions provide a permeability barrier at the boundary between the apical and lateral plasma membrane domains, and the desmosomes and adherens junctions serve to structurally support and stabilize the cell–cell contacts.

More than 85% of tumors in humans are carcinomas, that is, they are epithelial in origin. In many carcinomas intimate cell–cell contact is lost and the stereotypic array of epithelial junctions disappears. The cells become anaplas-

Address all correspondence to Drs. D. D'Urso, Neurologische Klinic, Neurochemisches Lab, University of Düsseldorf, Moorenstr. 5, 40225 Düsseldorf. Tel.: 49 211 311 89 84. Fax: 49 211 311 84 85; and David R. Colman, Brookdale Center for Molecular Biology, The Mount Sinai School of Medicine, One Gustave Levy Place, Box 1126, New York, NY 10029. Tel.: (212) 241-5775. Fax: (212) 423-0596.

1. *Abbreviations used in this paper*: CAM, cell adhesion molecule; NCAM, neural cell adhesion molecule; PNS, peripheral nervous system.

tic and pleiomorphic, and may readily metastasize. It has become clear recently that in these transformed cell populations, the presence of functional CAMs, that are known to play roles in the development and maintenance of adhesion processes in normal epithelial monolayers, may be inversely correlated with the degree of metastatic potential of the corresponding tumor cells (Birchmeier et al., 1991; Frixen et al., 1991; Vleminckx et al., 1991; Takeichi, 1993). For example, low levels of expression of E- and P-cadherin are found in carcinoma cell lines where extensive tumor invasiveness has been demonstrated (Frixen et al., 1991; Navarro et al., 1991; Vleminckx et al., 1991). From a therapeutic standpoint therefore, there is reason to believe that augmentation of functional Ca^{++}-dependent CAMs in carcinoma cells may be one key to reengaging the normal epithelial cell program through suppression of the transformed state.

We have been studying the functional properties of P_0, a transmembrane glycoprotein (M_r ~28,000) that mediates adhesion of Schwann cell plasma membrane surfaces to form compact myelin in the peripheral nervous system (PNS) of vertebrates. P_0 is a member of the immunoglobulin (Ig) gene superfamily of CAMs that contains a single variable-like region in its extracellular segment (Lai et al., 1987, Lemke et al., 1988). This, and an analysis of its exon-intron structure, have led to the suggestion that P_0 may possess adhesive properties similar to those of a primordial IgCAM from which all other members of this large superfamily may have arisen (Williams and Barclay, 1988). According to this view, a general role for an ancestral P_0-like IgCAM might have been to contribute to intercellular adhesion, essential for the development of multicellular organisms (Williams and Barclay, 1988). A primordial P_0-like IgCAM was probably highly adhesive, and homophilic, and in certain tissues of some early organisms may have formed extraordinarily stable intercellular bonds. The fact that P_0 expression in contemporary vertebrates is limited to myelinating cells may therefore not be surprising, since the compact myelin spiral, once formed, is not disassembled under normal conditions.

It has been demonstrated that after gene transfer P_0 can mediate pronounced cell–cell adhesion in a Ca^{++} independent manner (D'Urso et al., 1990; Filbin et al., 1990; Schneider-Schaulies et al., 1990). We have shown that when the protein is expressed by cDNA transfection in HeLa cells, a human cervical carcinoma, it becomes concentrated at the lateral intercellular boundaries between adjacent P_0-expressing cells (D'Urso et al., 1990). By confocal immunofluorescent microscopy, it was clear that P_0 expressors established very close, straight borders with each other. However, P_0 remained uniformly distributed in the plasma membranes of those expressors that were isolated from one another on the coverslip, or in those that made contact with control nonexpressors (see Fig. 5, D'Urso et al., 1990). A preliminary ultrastructural examination of confluent P_0 expressors suggested that at their plasma membrane appositions certain ultrastructural rearrangements took place. The loosely interdigitating finger-like processes observed in control cell populations were absent. Instead, a close (~5 nm), lengthy interface formed (D'Urso et al., 1990) that was reminiscent in its regular appearance and width of the intercellular gap of the intraperiod line of mature peripheral nerve myelin (Raine, 1984). We interpreted these data as evidence for pronounced cell–cell adhesion induced by the homophilic association of the extracellular segments of P_0 expressed on adjacent cell surfaces.

In this report, we show that HeLa cells generate a complex response to P_0-induced adhesion which greatly augments the placement of junctional proteins at cell–cell contacts, thereby compelling the assembly of certain junctional complexes, such as desmosomes and adherens junctions that are characteristic of normal epithelia. To our knowledge this is the first demonstration that a nervous system IgCAM, by obligating cells to adhere to one another, can trigger reversion of host tumor cells to an epithelioid phenotype. Our data raise the possibility that expression in carcinoma cells of any functional cell adhesion molecule that establishes close membrane apposition ultimately drives the cells to enhance the normal cell adhesion program such that stabilizing junctions are formed, and suppression of the transformed phenotype is achieved.

Materials and Methods

Cell Culture and Transfection

HeLa cells, a cell line derived from a human cervical carcinoma, were routinely cultured in DMEM supplemented with 7.5% FCS, 100 U/ml penicillin, 100 mg/ml streptomycin and 2 mM L-glutamine (all supplied by Gibco BRL, Gaithersburg, MD). To obtain clonal lines of P_0 expressors, HeLa cells were transfected with a cDNA encoding the full-length P_0 protein (Lemke and Axel, 1985). The P_0 cDNA was subcloned into the pECE vector (Ellis et al., 1986) and P_0pECE was introduced into the host HeLa cells along with the plasmid pSV2-neo (Southern and Berg, 1982) by liposome-mediated transfection as previously described (D'Urso et al., 1990). The day after transfection cells were split and seeded in complete DMEM containing 400 μg/ml of Geneticin G418 (Gibco) to select stable transformants. Cells transfected with the plasmid pSV2-neo only were used as control populations in all experiments. All stable transformants were maintained in culture in selection medium.

Unless otherwise noted, in each experiment, control cells and P_0 expressors were treated with 5 mM sodium butyrate, which has been shown to boost transcription of recombinant plasmids in mammalian cells (Gorman et al., 1983), and we have used extensively in previous work (D'Urso et al., 1990; Staugaitis et al., 1990; Allinquant et al., 1991). Butyrate treatment of nontransfected HeLa cells, and pSV2-neo–transfected cells did not induce epithelialization, as assessed morphologically or immunochemically with the markers we used in our studies.

Electron Microscopy

Stable P_0 transformants (pSV2-neo and P_0pECE cotransfected) and control cells (pSV2-neo only) were plated and grown in multiwell dishes. 24–48 h after becoming confluent, both control and P_0-transfected cells were treated with 5 mM sodium butyrate for 16 h (Gorman et al., 1983), which increases the level of expression of P_0 severalfold (see Fig. 1 *C–E*), after which they were washed with PBS, fixed with 2% paraformaldehyde and 2% glutaraldehyde in PBS, pH 7.2, for 1 h, postfixed in 2% OsO_4, and embedded in Epon before being processed for routine transmission electron microscopy. Ultrathin sections (0.6 μm) were cut perpendicular to the plane of the monolayer and contrasted with uranyl acetate and lead citrate.

Adhesion Assay

Confluent monolayers of P_0 expressors and control cells were cultured for 16 h in complete DMEM containing 5 mM sodium butyrate. The presence or absence of butyrate in control cell populations was not found to affect cell aggregation (data not shown). After replacing the media with complete DMEM minus butyrate for at least 3–5 h, cells were trypsinized and

reduced to single cell suspensions at a density of 10^6 cells/ml. Cells suspensions were maintained with constant stirring (2 rpm/s) at 37°C in a humidified atmosphere of 5% CO_2 and aggregates of cells formed by three or more cells were counted at time points (Fig. 2) using a hemocytometer. The assay was also performed in media containing 0.5 mM EGTA to chelate any residual Ca^{++} under otherwise identical conditions.

Antibodies

An affinity-purified polyclonal rabbit anti-P_o serum was used as previously described (D'Urso et al., 1990). The mouse monoclonal antibody we used recognized both desmoplakin I and II (Cowin et al., 1985). A guinea pig desmosomal cadherin antibody (anti-desmocollin/desmoglein, Mechanic et al., 1991) and rabbit anti-desmoglein (Schmelz et al., 1986) were used, and Dr. S. Citi provided the rabbit cingulin antibody (Citi et al., 1988). The tight junction associated protein ZO-1 was detected using affinity-purified serum obtained from Zymed Labs (S. San Francisco, CA) (Willott et al., 1992). A mouse monoclonal, clone RGE 53, specifically recognizing cytokeratin 18 (Ramaekers et al., 1983), was purchased (ICN Immunochemicals, Costa Mesa, CA). Antibodies against chicken A-CAM (GC-4, Volk et al., 1990), which cross-reacts with human N-cadherin, and mouse anti-vinculin (Goncharova et al., 1992), were purchased from Sigma Chem. Co. (St. Louis, MO). Dr. B. Gumbiner (Sloan-Kettering, New York) donated the mouse anti-α catenin serum.

Immunocytochemistry

Cells were plated on poly-L-lysine–coated coverslips, treated with butyrate (as above), and prepared for immunohistochemistry by one of the following procedures. For routine localization of P_o and N-cadherin in transfected HeLa cells, cells were washed with 0.2% gelatin/PBS and fixed (4% paraformaldehyde [PFA], 10 min, 23°C). Cells were then washed and permeabilized (0.05% Triton X-100, 100 mM PBS [pH = 7.4], with 0.2% gelatin added [PBS-gel]). Incubation with P_o antiserum was followed by several washes and treatment with fluorescent-conjugated secondary antibody. For localization of desmoplakin, desmocollin, desmoglein, cingulin, ZO-1, keratins, and α-catenin, cells were washed with PBS-gel, briefly (2 min) incubated in buffer I (140 mM NaCl, 1.5 M KCl, 10 mM Tris-HCl [pH = 7.4], 5 mM EDTA, 0.5% Triton X-100) to remove soluble proteins, and then immersed in ice-cold 100% methanol for 5–10 min. Incubations with primary and secondary antibody were then performed. This fixation treatment appeared to precipitate desmoplakin on the coverslip but completely obliterated any P_o immunoreactivity. To label both P_o and desmoplakin in the same cells, 1% paraformaldehyde was used for fixation and cells were incubated with both antibodies after permeabilization with 0.05% Triton X-100. Although this treatment allowed simultaneous localization of desmoplakin and P_o in cells, we noted that some P_o immunofluorescence was lost due to the low concentration of PFA used. For light microscopy, coverslips were mounted on slides in a solution of 2.5% DABCO (Sigma) in PBS with added glycerol.

A VANOX light microscope (Olympus Corp., Tokyo, Japan) was used for conventional immunofluorescence microscopy. For confocal analyses, both the Leica TCS (Fig. 2) and PHOIBOS 1000 (Sarastro, Inc., Sweden) (Fig. 6) confocal microscopes were used. Confocal image processing was performed as previously described (D'Urso et al., 1990), except for Fig. 2, in which data was initially stored on an IBM PC, transferred to a Silicon Graphics Indigo terminal, and volume rendered with Voxel View software. For volume rendering, 135 confocal sections, each section 0.1-μm thick and 256 × 256 pixels, were taken in the xy plane from a field of P_o-labeled cells. The volume rendered data was then rotated 90° in the y-axis and sections taken in the xz plane. For the data in Fig. 6, 512 × 512 pixel images were obtained to examine 0.8-μm optical sections.

RNA Isolation

Total RNA was prepared from confluent monolayers of controls and P_o expressors after overnight butyrate treatment. RNA isolation was performed by the guanidinium acid-phenol method (Chomczynski and Sacchi, 1987). RNA concentration in each sample was determined by measuring the absorbance at 260 nm and in all experiments the same amount of RNA was used for controls and P_o expressors. cDNA was synthesized with oligo$(dT)_{12-18}$ primers and the Moloney murine leukemia virus (M-MLV) H^- Reverse Transcriptase (Superscript, Gibco Brl). Reverse transcription was allowed to proceed at 42°C for 1 h, followed by a 5 min incubation at 99°C to inactivate reverse transcriptase. First-strand cDNA synthesized in this way was used as template for polymerase chain reactions (PCR).

PCR Amplification

Specific PCR primers that recognize sequences in the carboxyl-terminal domain of human desmoplakin (hd1 and hd2) were designed based on the published sequence (Green et al., 1990). The primers were: hd1 (upstream) 5′-TCAAGCTGCATAGCAGGCATATAC-3′; and: hd2 (downstream) 5′-GTAAGGGCTGGGTAAGCCCTTGGA-3′, that flank a 1,682-bp segment. For PCR quantitation, specific primers that amplify a stretch of 431-bp of the cDNA encoding the human glyceraldehyde 3-phosphate dehydrogenase (hgapdh) (Tokunaga et al., 1987) were used in parallel reactions to assess relative amounts of cDNAs added to each reaction mixture. These primers were: hgapdh1 (upstream): 5′-CTCATGACCACAGTCCATGCCATC-3′; and: hgapdh2 (downstream): 5′-TCGTTGTCATACCAGGAAATGAGC-3′. Aliquots of reaction mixture were removed at various points between 10 and 20 cycles and assessed for the presence and intensity of hgapdh bands on agarose gels.

To determine if there was a difference in the relative levels of desmoplakin mRNA in controls and P_o expressors, 10 ng of each cDNA template was subjected to PCR. All PCR experiments were performed in a Perkin-Elmer-Cetus Corp. (Norwalk, CT) DNA thermocycler. cDNA template was denaturated at 94°C for 1 min and annealed with hd1 and hd2 primers at 50°C for 2 min, the temperature was then ramped over 1 min to 74°C and elongation by Taq DNA polymerase in the buffer recommended by the manufacturer (Promega Corp., Madison, WI) supplemented with 2.5-mM $MgCl_2$ proceeded for 3 min. Amplifications were performed under identical conditions using hgapdh primers. For all PCR reactions, 5-μl aliquots were removed at cycles 8, 10, 12, 14, 16, 18, and 20). PCR products were visualized on 1% agarose gels. For autoradiography, 1 μCi [α-^{32}P]dATP (New England Nuclear, Boston, MA) was added to each PCR reaction and the newly synthesized DNA separated on 1% agarose gels. Gels were then dried and exposed on X-OMAT (Kodak) film. Densitometric analysis of autoradiograms was performed on a Computing Densitometer model 300A (Molecular Dynamics, Sunnyvale, CA).

To analyze the expression of mRNAs encoding molecules of the cadherin family in the transfected cells, degenerate oligonucleotides were designed. We chose two highly conserved amino acid sequences by comparing various homologous sequences within the family of the cadherin molecules (Hatta et al., 1988). The primers that amplify sequences encoding human N-cadherin (Reid and Hemperly, 1990) were: (upstream) 5′-GTIATIGA$^{T}/_{C}$ATGAA$^{T}/_{C}$GA$^{T}/_{C}$AA$^{T}/_{C}$$^{C}/_{A}$GICCIGA-3′; and: (downstream) 5′-AT$^{A}/_{G}$TCIGCIA$^{G}/_{A}$$^{T}/_{C}TT^{T}/_{C}TT^{A}/_{G}AAI^{C}/_{T}$$^{G}/_{T}$I-3′, where "I" is an inosine. PCR amplification was carried out in the same manner as described above. After PCR and electrophoresis, the 2,000-bp products in a single band were purified (Geneclean, BIO 101 Inc.), treated with Klenow polymerase (Promega) and blunt-end ligated into pGEM-7Zf(+) (Promega) at the single SmaI site. JM101 cells were transformed with the plasmid, 140 colonies containing insert were grown and DNA from each was purified using plasmid purification kits (Quiagen, Inc., Chatsworth, CA). Computerized automated sequencing of 21 cDNA inserts was performed on the model 373A DNA Sequencer (Appl. Biosystems, Inc., Foster City, CA).

The EMBL accession numbers for the cDNAs we used are as follows: human desmoplakin, J05211; human GAPDH, M33197; and human N-cadherin, X54315. Homology searches, sequence comparisons, and alignments were done with the University of Wisconsin Genetics Computer Group software on a VAX computer (Devereux et al., 1984).

Southern Blot Analysis

DNA amplified with the degenerate primers, using first strand cDNA from control cells and P_o transformants as a template, was separated on 1% agarose gel, denaturated (0.2N NaOH, 0.6 M NaCl) and transferred by capillary blotting to GeneScreen membranes (New England Nuclear) in 0.025 M Na_2HPO_4/NaH_2PO_4 (pH 6.5). Plasmid pGEM-7Zf(+) containing an insert encoding authentic human N-cadherin was linearized with BamHI and labeled with [α-^{32}P]dATP by random primer extension and used as probe (Feinberg and Vogelstein, 1983). The membrane was hybridized with the labeled probe (18 h 65°C in 1× SET [0.15 M NaCl, 0.03 M Tris-HCl, pH = 8, 0.02 M EDTA]), 10× Denhardt's solution, 0.1% SDS, 0.1% sodium pyrophosphate added. Blots were washed for 1 h at 65°C in 1× SET, 0.1% Na pyrophosphate, 0.1% SDS, and then 1 h at 65°C in 0.1× SET, 0.1% Na pyrophosphate, 0.1% SDS, before being exposed for auto-

radiography. Autoradiograms were analyzed by a Computing Densitometer model 300A (Molecular Dynamics).

Protein Preparation, SDS-PAGE, and Immunoblotting

Triton X-100 soluble and cytoskeletal fractions (Franke et al., 1981) of control and P_o-expressing HeLa cells were prepared as described. Briefly, cells were grown to confluency on 100-mm petri dishes, treated with 5 mM butyrate for 6–16 h, washed 3× with PBS, scraped off the dish, and pelleted (1,000 rpm, 5 min). Pellets were treated with 300 μl of lysis buffer (140 mM NaCl, 1% Triton X-100, 5 mM EDTA, 10 mM Tris [pH 7.4], leupeptin [0.5 μg/ml] and pefabloc [0.1 μmol]). After cell lysis, samples were centrifuged (15,000 *g*, 15 min), after which the supernatant was reserved and the pellet resuspended in a high salt extraction buffer (lysis buffer with 1.5 mM KCl and 0.5% Triton X-100 added). Insoluble cytoskeletal fractions were pelleted from this suspension (15,000 *g*, 15 min), and solubilized (1% SDS, 10 mM Tris [pH 7.4], 5 mM EDTA). Protein concentrations were determined with the BCA protein assay (Pierce, Rockford, IL), samples run on 7.5% SDS-PAGE, transferred to nitrocellulose, blocked with 5% milk protein, and incubated overnight with primary antibodies. After routine washing and secondary antibody incubations, blots were developed with the ECL chemiluminescence system (Biorad Labs., Hercules, CA).

Results

HeLa Cells Expressing P_o Become Polygonal and Exhibit Intercellular Concentration of P_o

HeLa cells were cotransfected with the vector pSV2neo (Southern and Berg, 1982) that encodes neomycin resistance, and a full-length rat P_o cDNA (Lemke and Axel, 1985) inserted into the vector pECE (Ellis et al., 1986) (P_opECE). Permanent cell lines of P_o expressors and control cells (PSV2neo transformed only) were established by a selection in G418-containing medium. As detailed in Materials and Methods, control and P_o expressors were treated with butyrate upon reaching confluency. Under these conditions, permanent P_o-expressing cells displayed a markedly different morphology from the control HeLa cells (Fig. 1, *A* and *B*). Under phase-contrast microscopy, control HeLa cells (Fig. 1 *A*) appeared spindle shaped and fibroblastic, with clearly defined phase-bright cell–cell borders. By contrast, P_o-expressing cells (Fig. 1 *B*) were flat and polygonal, and their cell–cell boundaries harder to discern, suggesting that these cells made closer contact than control cells. The morphological differences observed by us by phase microscopy closely resemble those reported by Mege et al. (1988), when S180 cells, a mouse sarcoma (nonepithelial) line, were transfected with L-CAM, the chick homologue of E-cadherin. In this study, L-CAM apparently was capable of interacting with specific intracellular components of the S180 cells (e.g., actin) and it was concluded that cell–cell adhesion mediated by L-CAM directly brought about these cytoarchitectural changes.

When monolayers of permanent P_o expressors were examined using conventional immunofluorescence, without butyrate treatment, we observed a low level of P_o immunoreactivity (Fig. 1 *C*), and moreover, as expected, that 6 h–18 h treatment with butyrate (5 mM) enhanced P_o expression severalfold in these cells (Fig. 1 *D*). While low levels of P_o were detected in noninduced expressors in cell extracts (Fig. 1 *E*, [−] lane), substantially greater levels (at least 10-fold) were found in butyrate-treated cells (Fig. 1 *E*, [+] lane). Thus both immunofluorescence and protein blotting clearly demonstrate butyrate induction of P_o expression.

The conventional immunofluorescence images revealed that P_o became concentrated at regions of cell–cell contact (Fig. 1, *C–D*), as we have documented previously (D'Urso et al., 1990). In fact, by confocal microscopy (Fig. 2), markedly elevated concentrations of the protein at the lateral cell–cell contact sites were found. Analysis of P_o localization was facilitated by volume rendering of sequential images in the xy plane and subsequent sectioning in the xz plane (Fig. 2 *B*, panels *1–8*). Using this approach, P_o localization was determined throughout representative cells in the monolayer. While some very low levels of P_o were found in the cytoplasm and at the free and basal cell surfaces, by far the highest levels of protein were found in regions where expressing cells made contact with each other (Fig. 2, panel *5*, *arrowheads*). As shown to be the case in our previous study (D'Urso et al., 1990), and consonant with studies on cadherin localization in transfected cells (Nagafuchi et al., 1987; Hirano et al., 1987; Mege et al., 1988), this pattern of protein distribution has been generally accepted as morphological evidence for cell–cell adhesion.

Cell Surface Junctional Complexes Become Prominent in P_o-expressing HeLa Cells

Permanent cell lines expressing P_o and control cells were grown to confluency and processed for transmission electron microscopy. Ultrastructural analysis of confluent monolayers of control cell populations revealed that the plasma membranes of adjacent cells rarely formed recognizable contacts with each other. Usually, contact was limited to membrane interdigitations (Fig. 3 *A*), although occasional small desmosomes or adherens junctions could be identified between some cells (Fig. 3 *B*, *arrow*). In stable lines of P_o-expressing HeLa cells, however, evidence for close association between adjacent cells was commonly obtained. In monolayers grown to confluence and maintained for 24 h, membrane protrusions were largely restricted to cell surfaces facing the medium, and for the most part were not present at the lateral intercellular borders. Instead, zones of close contact that exhibited electron-dense submembranous plaques and associated filaments were readily observed along these surfaces (Fig. 3 *C*, *arrows*). Between many cells, apical densities were noted (Fig. 3 *C*). These densities probably represented tight junctions, but frequently appeared "fused with", and therefore could not be resolved from, adherens-type junctions (Fig. 3 *C*, *arrows*). In sections cut perpendicular to the plane of the coverslip so that the entire lateral domain could be sampled, these contacts were variable in length and in extent of development. Cells maintained for several hours longer (48 h) produced regular appositions along the entire lateral plasma membrane domain (Fig. 3, *D* and *E*). Electron dense plaques indicative of developing adherens junctions and desmosomes (Fig. 3 *D*, *arrow*, and 3, *E* and *F*) could be readily detected in these regions.

We concluded that P_o expressors form broad zones of close contact between each other. In addition, we inferred that these initial contacts and the ensuing development of junctional elements (Fig. 3, *D–F*), detected by electron mi-

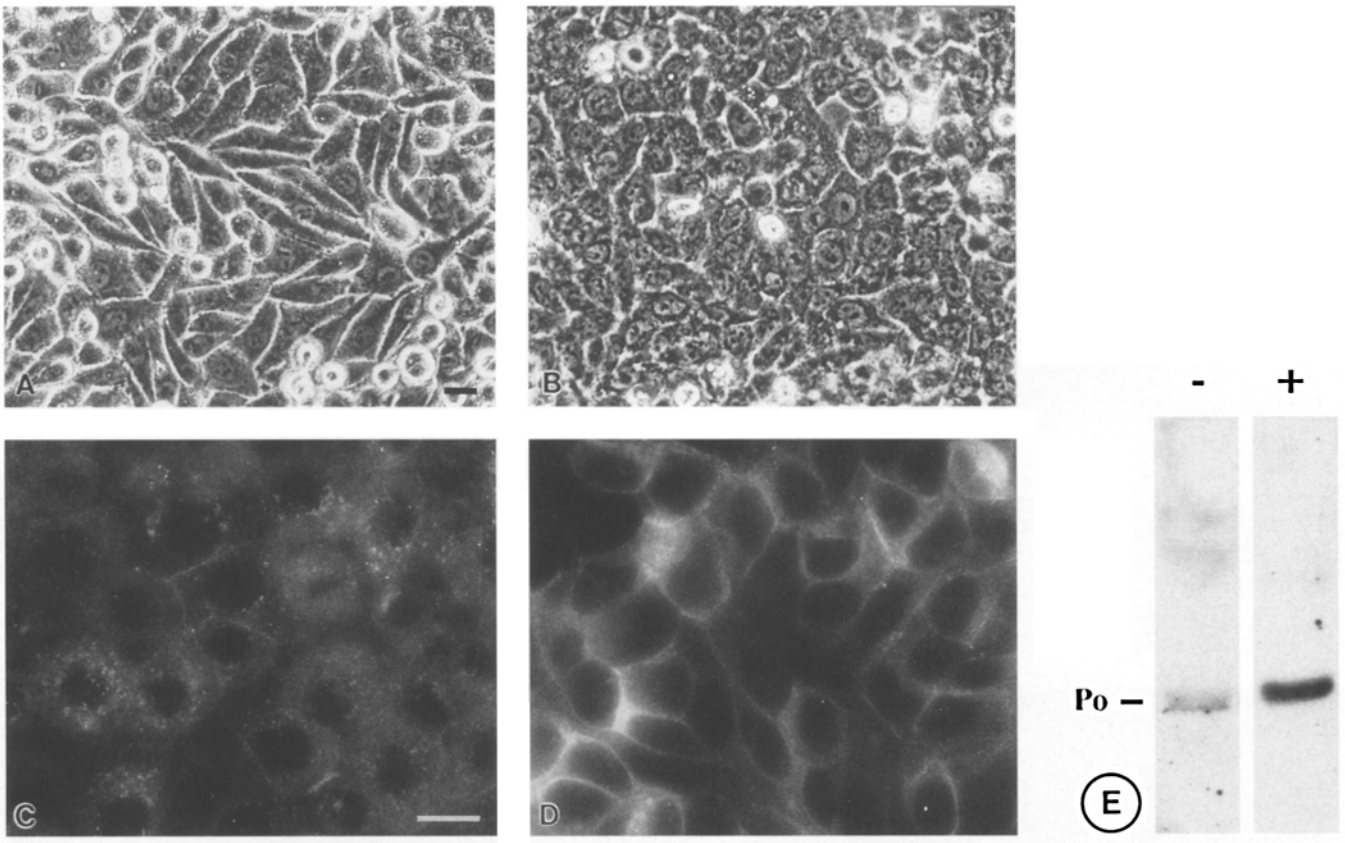

Figure 1. P_o expressors exhibit morphological changes and lateral localization of P_o protein. Phase contrast images of confluent monolayers of (*A*) control PSV2 and (*B*) P_o-expressing HeLa cells. Whereas control HeLa tend to be rounded and spindle shaped with distinct boundaries and obvious intercellular distances, P_o expressors are polygonal and cell–cell contacts appear close, almost fused in some cases. (*C* and *D*) Monolayers of permanent P_o expressors labeled for P_o. Cells without butyrate treatment (*C*) have a low level of P_o expression; addition of butyrate for 6–18 h substantially increases P_o expression (*D*). In both cases, P_o appears concentrated at lateral cell–cell contact sites. (*E*) Triton-soluble fractions of noninduced (−) and induced (+) P_o expressors are run on 7.5% SDS-PAGE (200 μg/lane), transferred to nitrocellulose, and probed for P_o using affinity purified antiserum. The noninduced cell fraction contains very little P_o protein relative to the induced cell fraction. The (−) lane was exposed 5× longer (by chemiluminescence) than the (+) lane. Bar, 20 μm.

croscopy, was indicative of a complex cellular response to cell–cell adhesion that merited further investigation.

P_o Expressors Rapidly Aggregate in Suspension

To directly determine whether P_o was acting physiologically as an adhesion molecule in this system we employed a classic adhesion assay (Brackenbury et al., 1977) that measures the capacity of single cells to aggregate over time when suspended at low density in Ca^{++} free medium.

HeLa cells grown to confluence and butyrate treated were used in this assay. In stable lines of P_o transformants the polypeptide can be readily detected by indirect immunofluorescence at the lateral borders between cells in the monolayer (Fig. 4 *A*). Mild trypsinization yielded >98% single cell suspensions of control (not shown) and P_o-expressing cell populations (Fig. 4 *B*) that were washed free of protease and maintained at low density (10^6 cells/ml) in Ca^{++} free medium with constant stirring. Although intracellular P_o glycoprotein was apparent by immunofluorescence in the trypsinized expressor cells (Fig. 4 *B*), as expected, protease treatment rendered the molecule undetectable at the cell surface. Within 15 min of incubation, however, small aggregates consisting of 2–4 cells were readily observed by phase microscopy in the P_o-expressing population, and on immunostaining, intense P_o immunofluorescence was detected at cell surfaces and was markedly concentrated at cell–cell interfaces (Fig. 4 *C*). Clearly, the internal pool of P_o that was protected from trypsinization, and/or newly synthesized P_o had reached the cell surface during this short time interval, where it homophilically mediated the development of cell aggregates. During the course of the experiments, the cellular aggregates in the P_o expressing population became quite large (Fig. 4 *D*), and the number of cells participating in aggregates was always far greater than in the control cell population (Fig. 4 *E*). For example, after 210 min of incubation, 55% of the P_o expressors were in aggregates, as compared with 22% of the controls.

These experiments show that once P_o reaches the HeLa cell surface, expressors begin to aggregate within minutes. The fact that P_o is found highly concentrated at the sites of cell–cell contact in the aggregates, and that cell aggregation can occur under Ca^{++} free conditions, argues that P_o

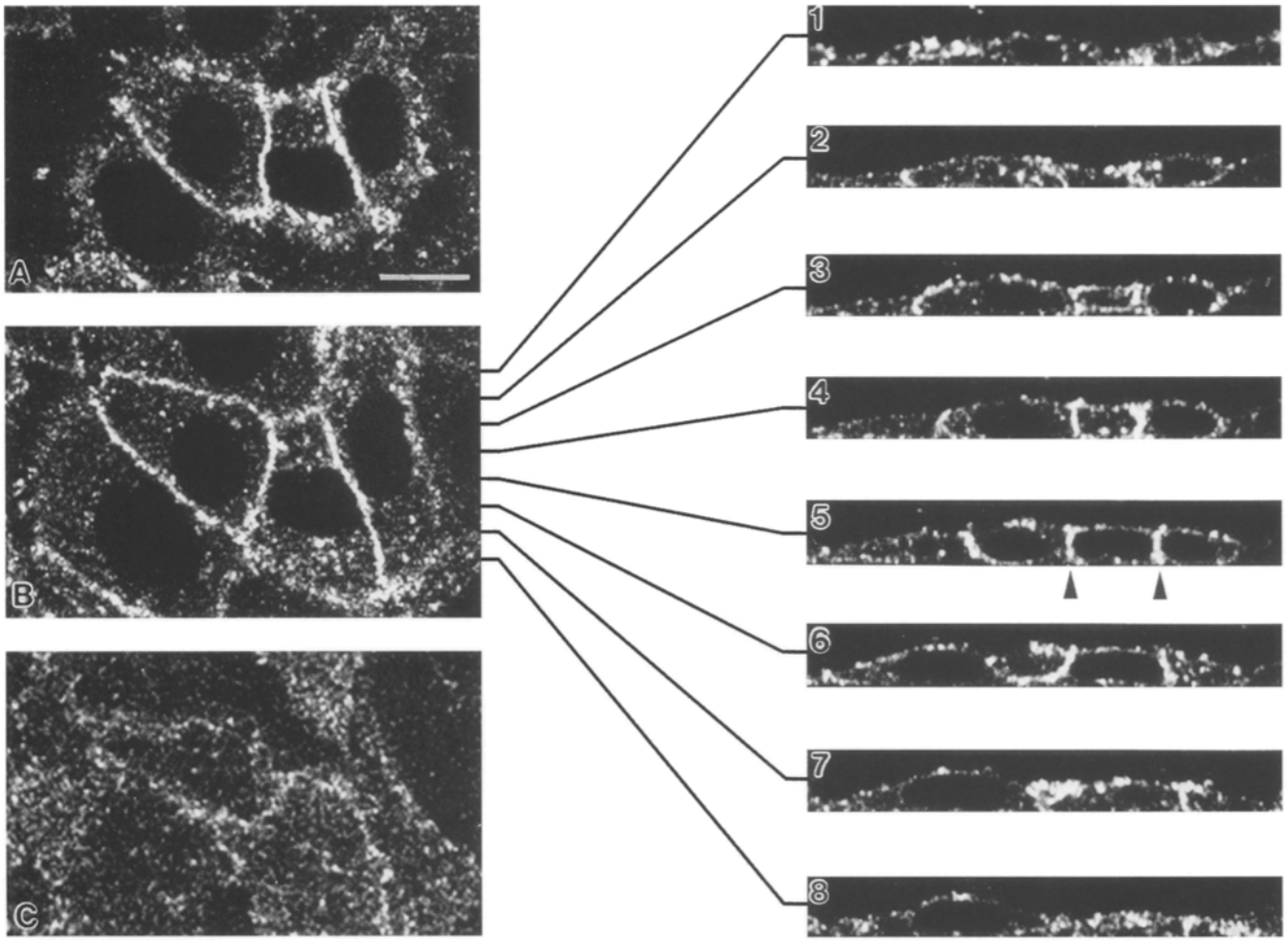

Figure 2. Localization of P_o protein by confocal microscopy. (*A*, *B*, and *C*) Confocal series of P_o-labeled expressors and corresponding xz sections from volume rendering of xy data. The images on the left are optical sections sampled 4-μm apart, from apical surface (*A*) to the coverslip level (*C*) of the cells. (*B*) Each xz image (3.5-μm apart) is connected by a line to the corresponding position on the xy image. P_o protein localization can therefore be followed from bottom to top, and through the full thickness of each cell. P_o is present in the cytoplasm and at the cell surface, but highly concentrates at cell–cell contact sites (*arrows*). Bar, 10 μm.

is the initiator of cell adhesion in this system, and that other known adhesion molecules such as members of the cadherin (Damsky et al., 1983; Ozawa et al., 1989; Takeichi, 1991) and integrin families (Albelda and Buck, 1990; Hynes, 1992) are not initially involved.

Tight Junctional and Desmosomal-associated Proteins Localize to Intercellular Boundary Regions between P_o Expressors

Ultrastructural analysis of P_o-expressing cells (Fig. 3) indicated that a remarkable response to P_o-induced adhesion that developed over time across extensive areas of the monolayer was the formation of junctional complexes. To begin to study the physiological parameters of this response, we examined eight known representative polypeptide constituents of these junctions.

We used antibodies against *cingulin* and *ZO-1*, proteins which are believed to be associated with tight junctions (Stevenson et al., 1986; Anderson et al., 1988; Citi et al., 1988), and *desmoplakin*, *desmocollin*, and *desmoglein*, (Cowin and Garrod, 1983; Cowin et al., 1985; Schmelz et al., 1986; Green et al., 1990) polypeptide components of desmosomes, to map the distribution of these structures across monolayers of P_o expressors and control cells grown in normal (i.e., calcium-containing) medium.

Cingulin is a cytoplasmic protein restricted to the subapical region of epithelial cells where tight junctions are found (Citi et al., 1989). In control cell populations of pSV2-neo transformants, cingulin immunoreactivity was distributed in a discontinuous, dot-like pattern. Rarely, short linear stretches of immunofluorescence were detected (Fig. 5 *A*, *arrows*) but for the most part, no clearly defined organization was discernible. In contrast, P_o expressors exhibited strong immunofluorescence selectively localized at the subapical regions of cells that were in contact with each other. Cingulin was usually distributed in what appeared to be a thin, continuous belt (Fig. 5 *B*) that under high magnification could often be resolved into parallel belts (Fig. 5 *C*, *arrows*), each of which probably local-

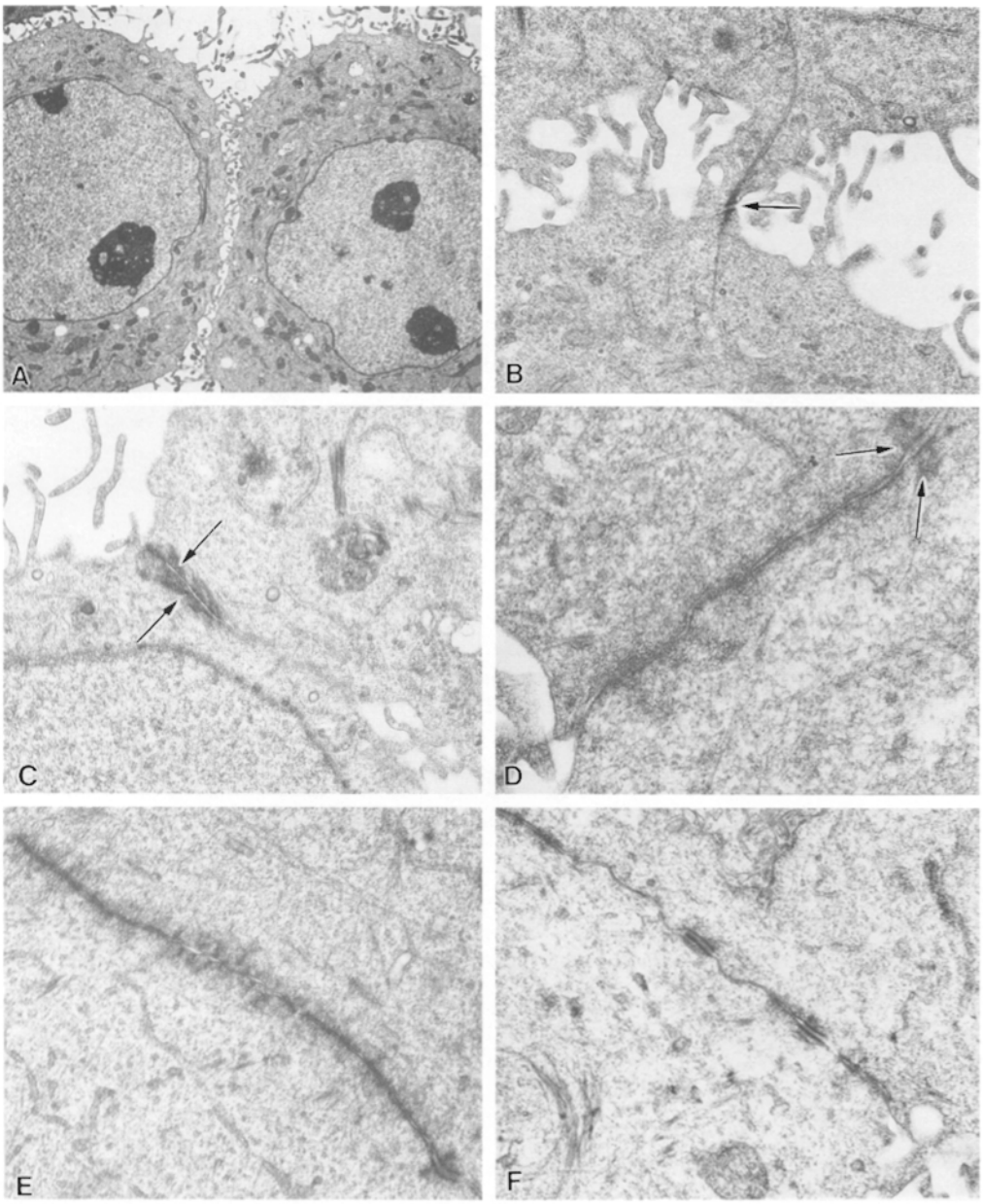

Figure 3. Development of junctional specializations in P_o transformants. Transmission electron micrographs of confluent, sodium butyrate-treated monolayers of (*A* and *B*) control cells and (*C*, *D*, *E*, and *F*) stable P_o transformants. At the borders of control cells interdigitating microvilli (*A*) and rarely, small desmosomes (*B*) can be observed. In contrast, within 24 h postbutyrate treatment, (*C*) adjacent plasma membranes of P_o expressors begin to develop apical subplasmalemmal densities (*arrows*). By 48 h, lateral domains display broad appositions (*D* and *E*) adherens junctions, and desmosomes. Desmosomes are clearly visible (*D*, *arrows*, and *F*). Bars: (*A*) 0.5 μm; (*B–F*) 0.1 μm.

ized under adjacent cell membranes. Another cytoplasmic protein found associated with tight junctions, as well as at cell–cell contacts of certain nonepithelial cell types, (Anderson et al., 1988; Stevenson et al., 1986; Howarth et al., 1992, 1994), is ZO-1. This protein showed a pattern of distribution similar to cingulin; in control cells (Fig. 5 *D*), ZO-1 was occasionally found at cell–cell contact sites, whereas ZO-1 immunofluorescence accumulated quite extensively at the membranes of P_o-expressing cells (Fig. 5 *E*). The distribution of these tight junction–associated proteins and P_o did not overlap; cingulin and ZO-1 were always detected in a narrow band above (i.e., "apical" to) the uppermost level of P_o reactivity and so the position of the cingulin and ZO-1 belts denotes the boundary below which P_o concentrates, and other junctional structures form (see below).

The aggregation experiments, taken together with the timed ultrastructural studies, suggested that adhesion mediated by P_o was a prerequisite for subsequent junction formation. We therefore directly examined the time course of appearance of desmosomes relative to the development of high levels of P_o fluorescence along intercellular borders. Cells were grown in medium containing Ca^{++}, which is required for desmosome assembly (Hennings and Holbrook, 1983; Mattey and Garrod, 1986; Mattey et al., 1990), and after fixation, processed for immunofluorescence with P_o and desmoplakin antibodies.

The desmoplakins are a set of closely related polypeptides (M_r ~215,000–250,000) that are found in association with the desmosomal plaque, where they may function in anchoring intermediate filaments to the plasma membrane (Cowin et al., 1985; Schwarz et al., 1990; Stappenbeck and Green, 1992; Garrod, 1993). Desmoplakin immunoreactivity is maximally visualized when cells or tissues are pretreated with 100% methanol; however, this agent was found to extract P_o from cell membranes. Although P_o im-

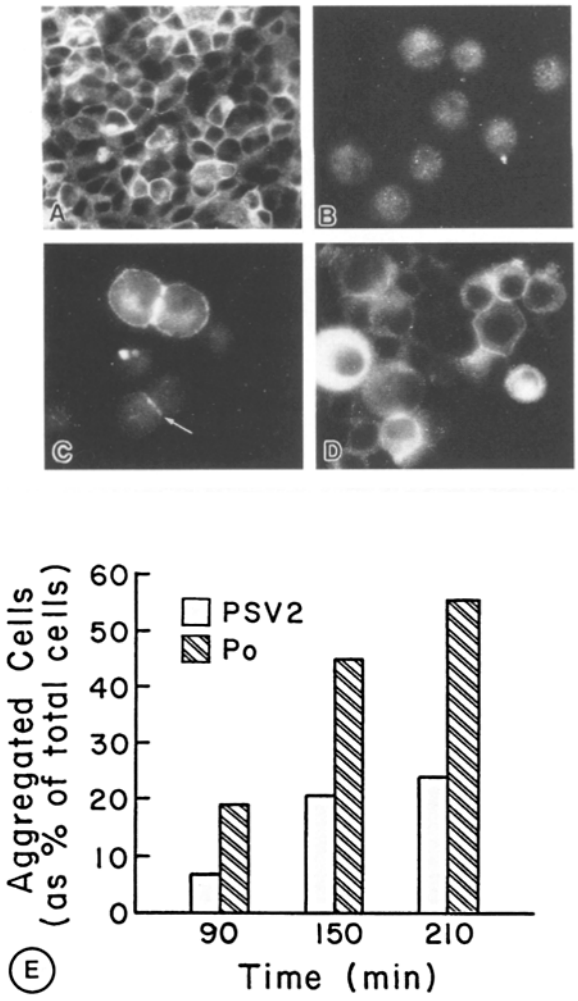

Figure 4. P_o expression enhances aggregation of cells in suspension. Indirect immunofluorescence of P_o transformants. (*A*) In confluent monolayers before trypsinization, P_o is localized to lateral cell borders. (*B*) In single cell suspensions of P_o expressors after trypsin treatment, cytoplasmic P_o immunostaining can still be observed. (*C*) By 15 min, cell aggregates form, and P_o immunofluorescence is predominantly concentrated at cell–cell contact sites even in low level expressors (*arrow*). (*D*) With time, the aggregates become much larger. (*E*) Aggregation was quantitated in a classic adhesion assay. HeLa cell controls (*unshaded*), or stable P_o expressors (*shaded*) were trypsinized briefly in PBS (Ca^{++}, Mg^{++} free), washed extensively in medium, mechanically disrupted and resuspended. The cell suspensions were maintained at 37°C for 3.5 h. Constant stirring was applied, and by hemocytometry, single cells represented 100% of the cell population at the starting time point. Aliquots were taken in triplicate at each time point, and the number of clumped cells (in aggregates of two or more) were counted and expressed as a percentage of the total cell population. P_o expressors tend to form adhesive clumps of cells much more readily than do the control cells.

munostaining in these cells is also greatly reduced when fixed with 1% paraformaldehyde, this milder fixation did allow us to localize both P_o and desmoplakin on the same coverslip. At early time points postbutyrate treatment, P_o immunofluorescence was detectable, but desmoplakin immunoreactivity was not apparent until several hours later. In fact, in many instances, P_o was detected completely concentrated in a continuous "island" or zone along entire intercellular boundaries (Fig. 6, *A* and *D*). Desmoplakin, by contrast, was distributed in regular dot-like arrays, presumably representing individual desmosomes in the process of formation, in discrete regions within the P_o adhesion island (Fig. 6, *B* and *C*). Eventually, rows of desmoplakin fluorescence, frequently double rows, developed within the P_o adhesive zone (Fig. 6, *E* and *F*).

The striking contrast between desmoplakin immunofluorescence detectable at the cell surface in the P_o expressors as compared with control cells is dramatically demonstrated by confocal microscopy (Fig. 6, *G* and *H*). In confluent control cell populations (Fig. 6 *G*), occasional short rows of isolated desmoplakin reactivity are identified (*arrows*). This is expected, since by thin-section electron microscopy, isolated fully developed desmosomes were occasionally observed between these cells (Fig. 3 *B*). Desmoplakin immunofluorescence of the confluent P_o expressors (Fig. 6 *H*) is so pronounced however that individual cell outlines can be readily appreciated. Immunofluorescence for desmocollin and desmoglein (Fig. 7), integral membrane proteins involved in the adhesive interaction of desmosomes (Goodwin et al., 1990; Holton et al., 1990; Koch et al., 1990; Cowin and Brown, 1993; Garrod, 1993), exhibited a dramatically increased distribution at the lateral cell membranes of P_o expressors. The immunofluorescence for desmosomal cadherins was particularly impressive, in that it outlined cell perimeters (Fig. 7 *D*). Taken together, these results argue that P_o-mediated adhesion leads to increased desmosome formation in HeLa cells.

The Adherens Junction-related Proteins N-Cadherin, α-Catenin, and Vinculin, Become Markedly Enhanced and Organized at Cell–Cell Contact Sites of P_o Expressors

In normal epithelia, adherens junctions may be found immediately subjacent to the apical tight junctions. A number of polypeptides involved in adherens junction formation have been identified (Geiger and Ayalon, 1992; Tsukita et al., 1992), including cadherins (Boller et al., 1985; Volk and Geiger, 1986*a*,*b*), catenins (Herrenknecht et al., 1991; Nagafuchi et al., 1991), vinculin (Geiger, 1979; Tsukita et al., 1992), and ZO-1 (Itoh et al., 1993 , and see above). Cadherins may play "instructive" roles in the establishment of cell–cell adhesion (Doherty et al., 1991), and it has been suggested that E-cadherin expression is a prerequisite for junction formation (Gumbiner et al., 1988). Both N- and E-cadherins have been identified in adherens junctions (Boller et al., 1985; Volk and Geiger, 1986*a*, *b*; and see Geiger et al., 1987), and are distributed as well across nonjunctional plasma membrane surfaces; normally, however, HeLa cells express very low levels of N-, but not E-cadherin (Ozawa et al., 1989; Herrenknecht et al., 1991; Knudsen, K. A., personal communication, and this study, see below). We therefore asked whether the organization of N-cadherin into adherens junctions might be affected by P_o-initiated cell adhesion.

N-cadherin antiserum (Volk et al., 1990) prominently labeled plasma membrane surfaces of expressors (Fig. 8 *B*), but not of control cells (Fig. 8 *A*). The immunofluorescence was extensively concentrated at lateral cell–cell boundaries in a continuous pattern, although puncta of fluorescence, probably corresponding to adherens junctions, were

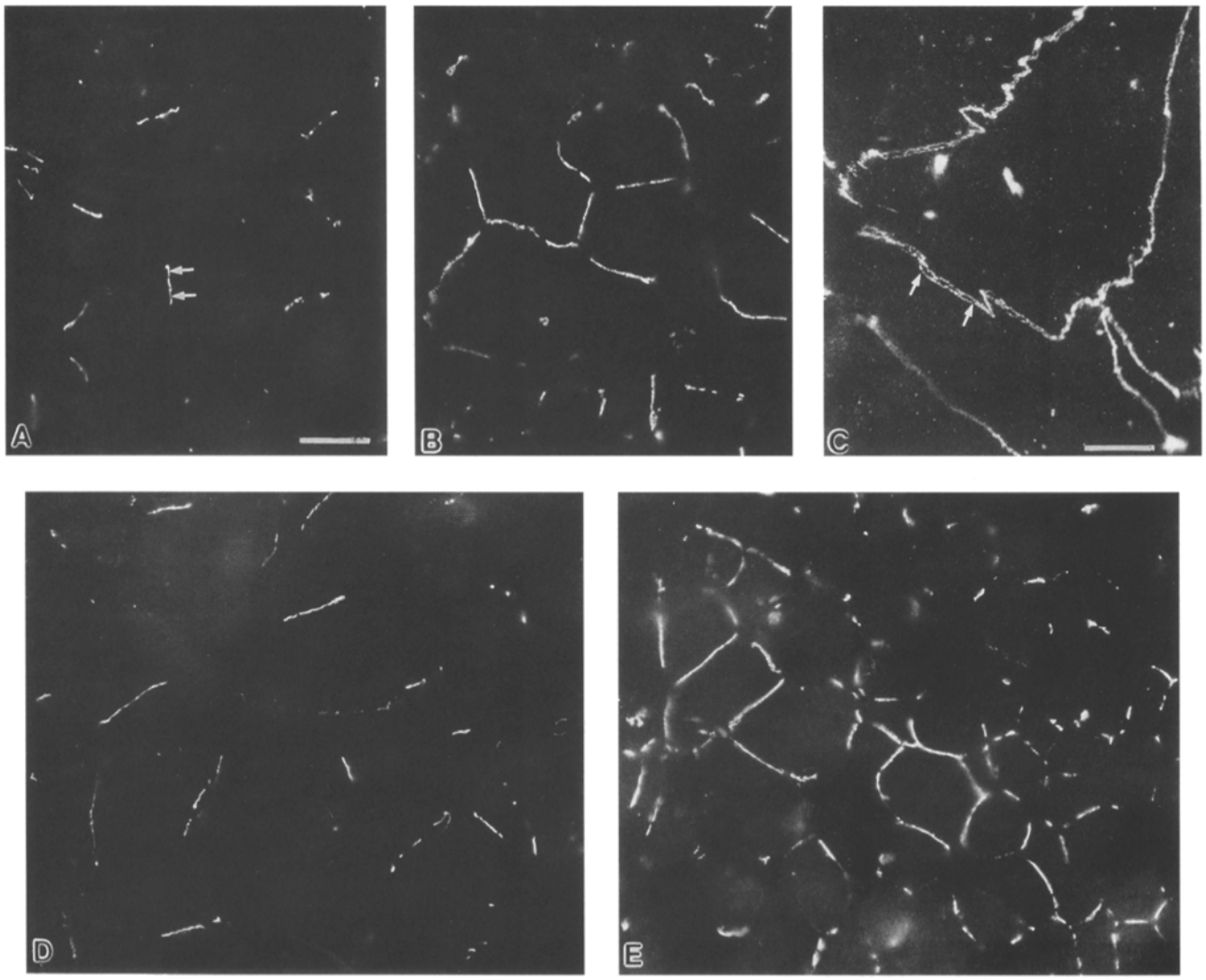

Figure 5. The tight junction–associated proteins cingulin and ZO-1 become highly organized at the cell surface. Cingulin immunofluorescence of (*A*) control PSV2-neo transformants and (*B* and *C*) P_o expressors. (*A*) In control cell populations, cingulin is sparsely detected along apical plasma membrane segments (*arrows*), but is distributed along the entire apical cell perimeter of P_o expressors (*B*), where at higher magnification, it may sometimes be resolved into two parallel belts (*C*, *arrows*). Likewise, while small stretches of control PSV2 cells are ZO-1 positive (*D*), P_o-expressing cells demonstrate extensive ZO-1 labeling at apical cell contact sites (*E*). Bars: (*A*, *B*, *D*, and *E*) 20 μm; (*C*) 2 μm.

plainly visualized. When specific antiserum raised against E-cadherin (Fannon et al., 1995) was used, no labeling in either control or P_o expressors was detected (not shown).

α-Catenin, a member of a family of cytoplasmic molecules which are found in association with the classic cadherins (Ozawa et al., 1989; Herrenknecht et al., 1991; Hinck et al., 1994; Nagafuchi et al., 1994; Nathke et al., 1994; Watabe et al., 1994), has been found experimentally to be important for junction formation. It has been postulated that the set of catenins, perhaps in coordination with certain unrelated cytoplasmic polypeptides (Ozawa et al., 1989; Cowin and Brown, 1993; Gumbiner, 1993; Hinck et al., 1994; Nagafuchi et al., 1994), regulate intercellular adhesion by mediating linkage of cadherins with the cytoskeleton. The P_o expressors were found to have markedly enhanced amounts of α-catenin (Fig. 8 *D*) at the cell surface, as compared with the controls (Fig. 8 *C*).

Vinculin is a cytoplasmic protein associated with adherens junctions and focal contacts whose role, like α-catenin, may possibly be to link adherens junction associated cadherins to the cytoskeleton (Geiger, 1979; Geiger et al., 1987; Geiger and Ayalon, 1992; Tsukita et al., 1992). Vinculin was found in focal contacts at the substrate level of both control and P_o expressors (not shown). However, in agreement with its putative role in cadherin adhesion, and with our results above, no vinculin labeling was found when focusing above the substrate in control cells (Fig. 8 *E*), but vinculin was clearly organized at the lateral borders of P_o expressors (Fig. 8 *F*) above the substrate.

Desmoplakin, N-Cadherin, and α-Catenin Are Relatively Increased in Response to P_o-mediated Cell Adhesion

The marked increase of desmoplakin immunofluorescence at the plasma membrane of confluent P_o expressors could

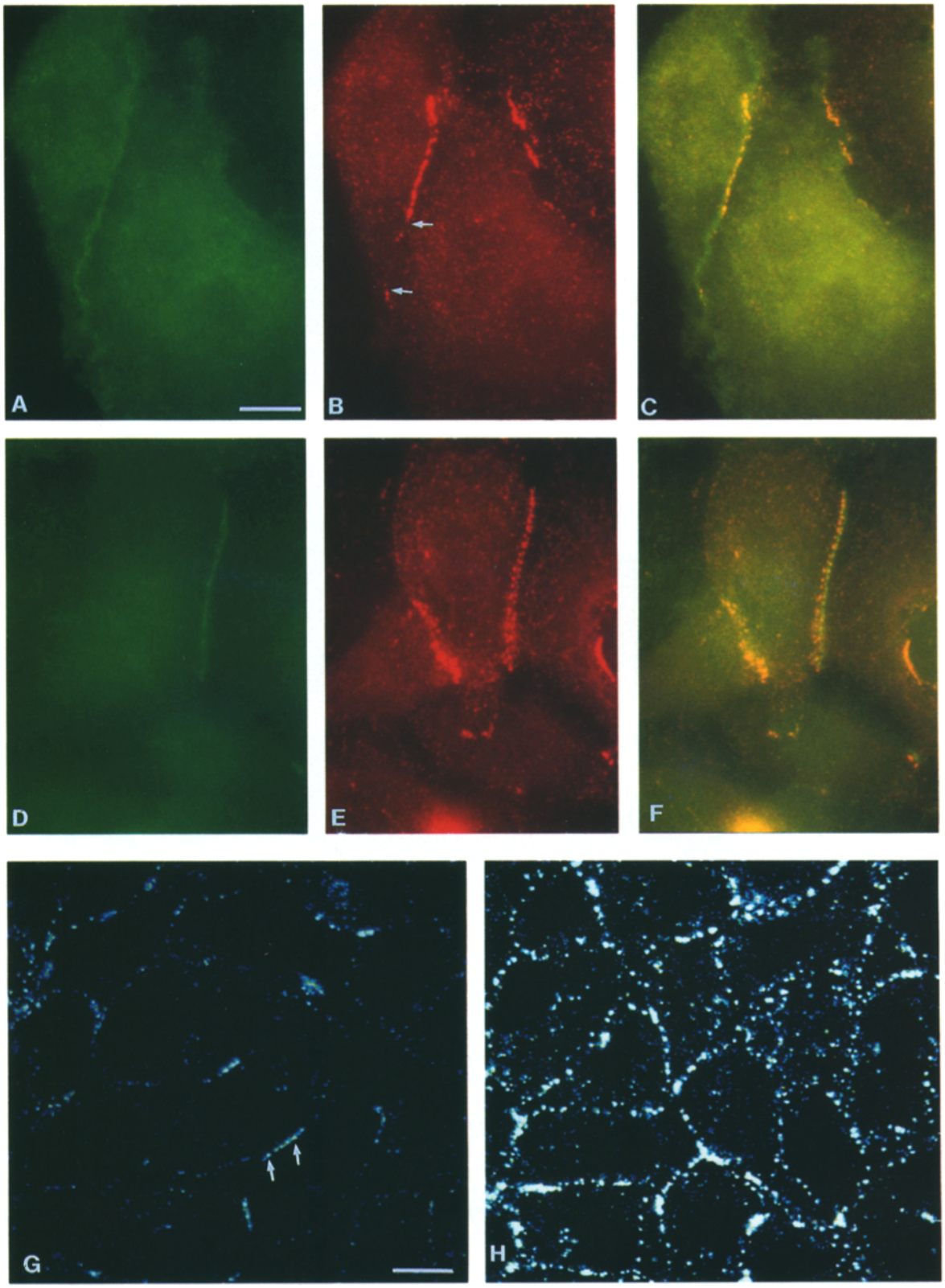

Figure 6. Desmoplakin and P_o colocalize at adhesive cellular interfaces. (*A–F*) P_o expressors on coverslips were simultaneously labeled with P_o and desmoplakin antibodies. At short time intervals (within 24 h; *A*, *B*, and *C*), P_o is found concentrated between neighboring cells. In the same cells, desmoplakin is in linear arrays that are not yet completely continuous. In *B*, the arrows indicate a plasma membrane segment that at all levels of focus contains P_o (see *A*) but is devoid of desmoplakin. In *C*, both P_o and desmoplakin are revealed. At later time points (up to 48 h), linear bands of desmosomes are revealed by desmoplakin immunofluorescence (*E* and *F*). By confocal microscopy (*G*), control cells exhibit little desmoplakin at the cell surface (*arrow*). By contrast, P_o transformants express so much desmoplakin that cell outlines are readily discerned (*H*). Bars: (*A–F*) 2 μm; (*G* and *H*) 10 μm.

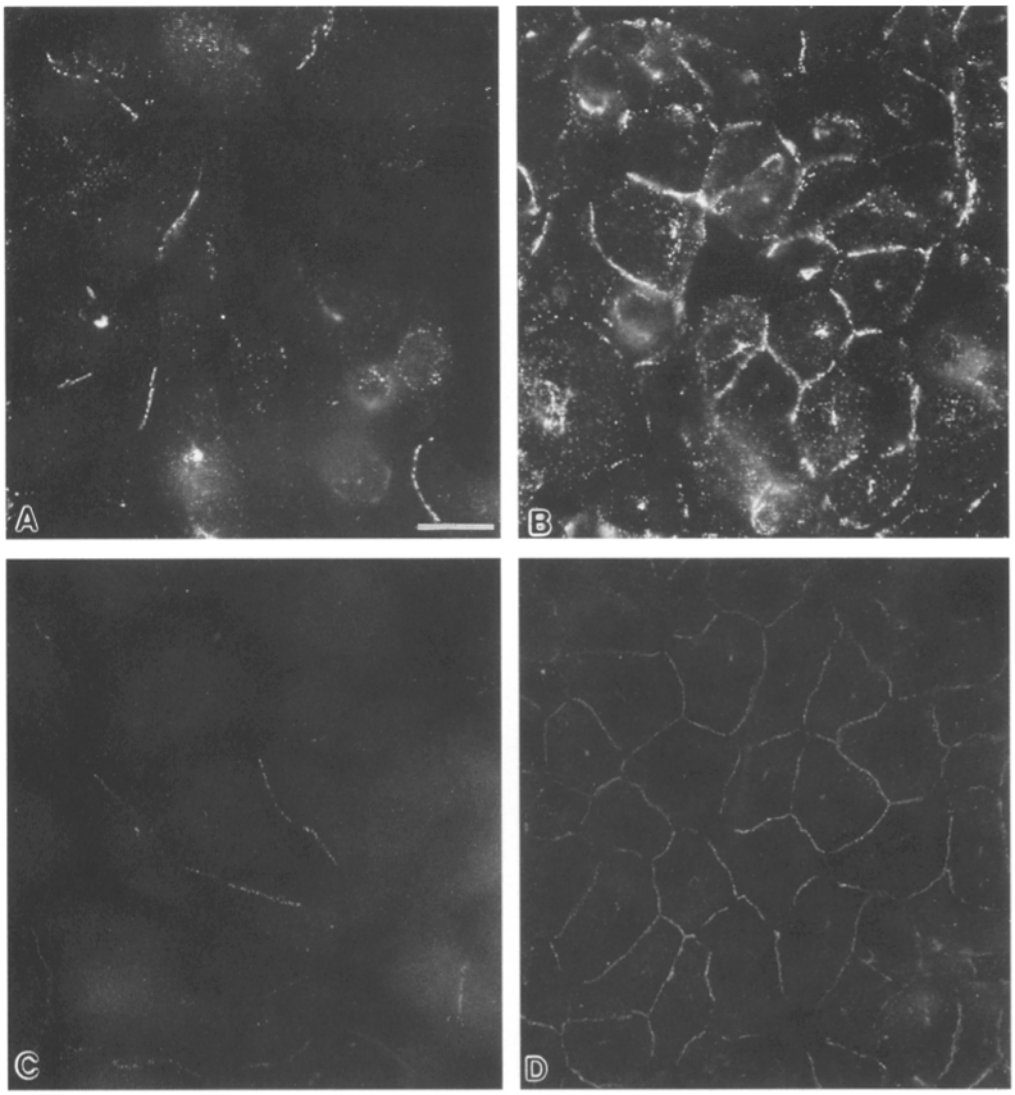

Figure 7. The desmosomal-associated integral membrane proteins, desmocollin and desmoglein, also organize in P_o expressors. (*A–D*) In addition to desmoplakin, the desmosomal proteins desmocollin and desmoglein are also found to localize at cell contact sites. pSV2 control cells (*A*) have very sparse desmoglein immunofluorescence at cell contact sites, in contrast to the extended distribution of this protein in P_o expressors (*B*). Desmocollin/desmoglein immunofluorescence is very limited in control HeLa cells (*C*), but is much greater in P_o expressors (*D*), clearly outlining cell boundaries. Bar, 20 μm.

be the result of stabilization of the protein at the surface, an increase in the transcription rate of the desmoplakin gene, and/or stabilization of the desmoplakin mRNA. According to the current literature, it is generally believed that the formation of desmosomes between cells is accompanied by a reduction in the rate of proteolytic breakdown of a relatively constant pool of soluble desmosomal polypeptide components, including desmoplakin (Pasdar and Nelson, 1988*a*,*b*; Pasdar et al., 1991). If this were so, it might be expected that equivalent relative mass amounts of desmoplakin mRNAs would be observed in control and expressing cell populations. If, on the other hand, the appearance of desmoplakin at high density at the cell surfaces of P_o expressors was the result of an increase in gene transcription or a stabilization of desmoplakin mRNAs, then an increase in the relative levels of these specific mRNAs would be detected in the confluent expressors.

To begin to address this in a preliminary way, we synthesized first-strand cDNA from total RNA prepared from confluent control cells or P_o expressors. Equivalent amounts of control and P_o expressor cDNA (~10 ng/reaction) were then used as templates in PCR reactions containing human desmoplakin specific oligonucleotide primers, and [α^{32}P]dATP as a source of label for quantitation. To ensure that equivalent amounts of control and expressor cDNA template were used in these experiments, some reactions were primed with oligonucleotides specific for human glyceraldehyde 3-phosphate dehydrogenase (GAPDH), a gene whose mRNA levels have been shown to be constant under a variety of conditions, and therefore has become useful in standardizing PCR reactions (not shown, but see Materials and Methods).

In these experiments, autoradiographs of agarose gels in which aliquots from several cycles (cycles 8–30, were routinely sampled) were displayed revealed, as expected, single bands of 1,682 bp, corresponding to the predicted length of the segment flanked by the desmoplakin-specific primers (Fig. 9 *A*, lanes *1–4*). However, the intensities of those bands obtained in the reactions containing cDNA prepared from the P_o expressors were visibly stronger in the earlier cycles when the PCR reaction is not rate limited by reagent depletion (Fig. 9 *A*, lanes *2* and *4*) than in the control reaction mixture (Fig. 9 *A*, lanes *1* and *3*). Densitometric scanning of autoradiographs derived from five different sets of cDNA preparations used for these studies demonstrated at least 6-, and up to 10-fold as much label

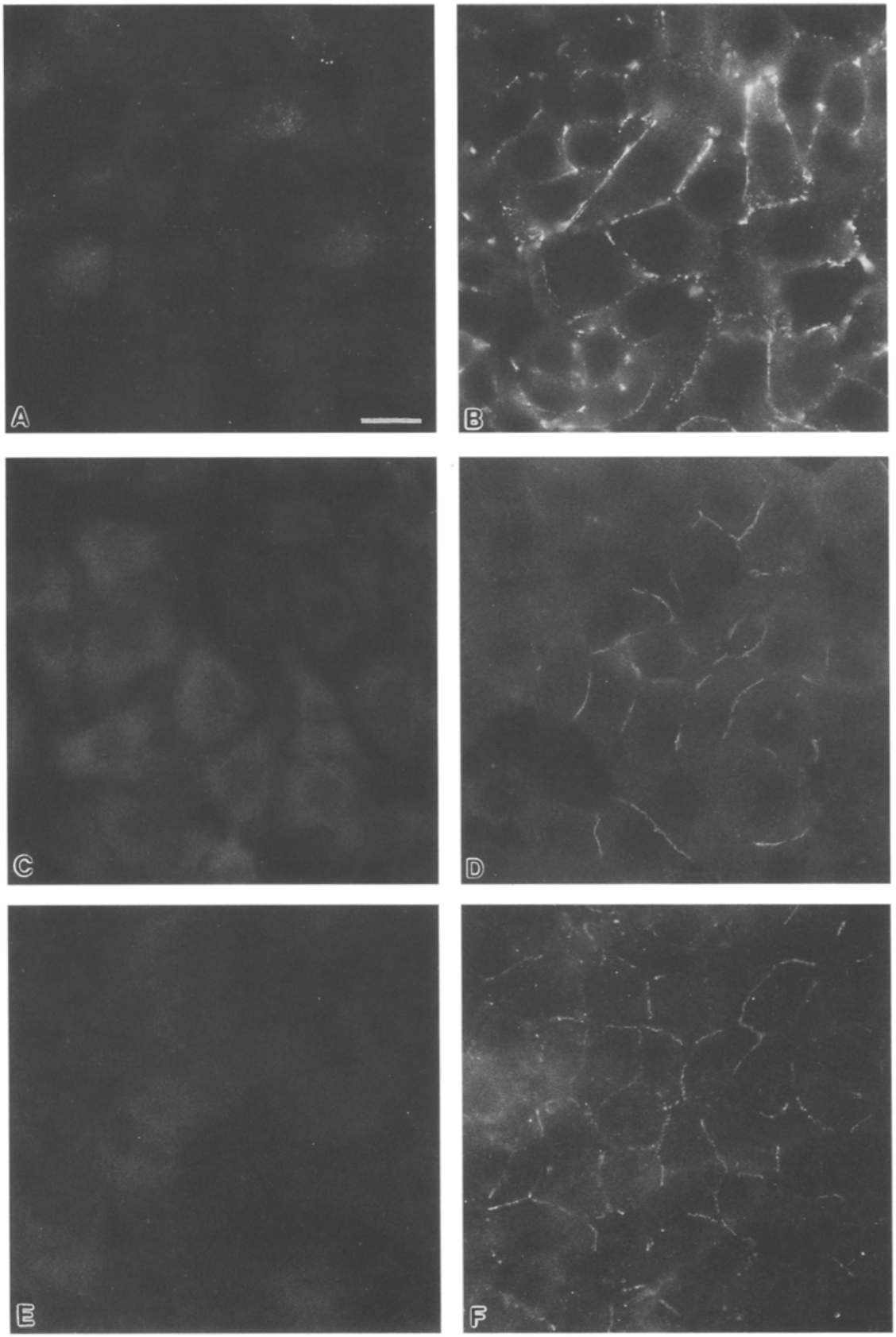

Figure 8. N-cadherin, α-catenin, and vinculin become localized to lateral cell–cell contact sites in P_o expressors. (*A–F*) Control and P_o-expressing HeLa cells were plated on coverslips and prepared for immunohistochemistry after reaching confluency. Unlike control cells (*A*), cells expressing P_o (*B*) were found to have substantial amounts of N-cadherin concentrated at lateral zones of cell–cell contact. Moreover, the cadherin-associated protein, α-catenin, was not detected in control HeLa cells (*C*), but was readily found at regions of membrane contact of P_o-expressing cells (*D*). Vinculin did not localize to apical cell contact sites of PSV2 cells (*E*), but did in P_o-expressing cells (*F*). These adherens junction-associated proteins were found to localize at the cell perimeters where expressing cells make contact, as did P_o, the desmosomal proteins, and the tight junction-associated proteins. Bar, 20 μm.

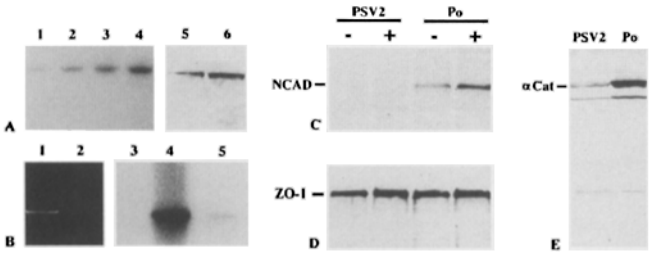

Figure 9. Levels of desmoplakin, N-cadherin and α-catenin are greater in P_o expressing HeLa cells than in control cells. (*A*) RT-PCR analysis of control and P_o-expressing HeLa cells using human desmoplakin primers (lanes *1–4*), and Western blot of cytoskeletal fraction of control and P_o-expressing HeLa cells using monoclonal anti-desmoplakin (lanes *5* and *6*). First strand cDNA from control (lanes *1* and *3*) or P_o-expressing cells (lanes *2* and *4*) was used in PCR reactions primed with human desmoplakin primers. [α-^{32}P]dATP was present in the reaction mixtures. After 14 (lanes *1* and *2*) and 16 (lanes *3* and *4*) cycles, 5 μl aliquots were run through an agarose gel and an autoradiograph was prepared.

Immunoblotting of the cytoskeletal fraction of induced control and P_o expressors (75 μg/lane) with a monoclonal anti-DP shows that DP levels are increased in P_o expressors (lane *6*) compared to control cells (lane *5*). (*B*) Ethidium bromide staining of PCR reactions carried out using first strand cDNAs synthesized from P_o (lane *1*) and pSV2-neo (lane *2*) HeLa transformants as template and degenerate oligonucleotides corresponding to common domains in N- and E-cadherin as primers. A single band was detected (lane *1*) in the P_o reaction expression mixture, while no band was detected from the pSV2-neo HeLa reaction (lane *2*). DNA blotting of the RT-PCR reactions using an [α-^{32}P]dATP human N-cadherin probe, using no template (lane *3*), P_o cDNA (lane *4*), or control pSV2-neo cDNA (lane *5*) as template. (*C*) In immunoblots of Triton-soluble extracts (200 μg/lane) of control (PSV2) and experimental (P_o expressing) HeLa cells, N-cadherin is detected in P_o-expressing cells, but not in control PSV2 cells, with (+) or without (−) butyrate. Levels of P_o are greatly enhanced in butyrate-treated cells (Fig. 1 *E*), as are levels of N-cadherin (+) compared to noninduced cells (−). (*D*) Relative levels of ZO-1 protein in cytoskeletal fractions (10 μg/lane) of control PSV2 cells and cells expressing P_o remain constant, with (+) or without (−) butyrate treatment. (*E*) On Western blots of cytoskeletal fractions (10 μg/lane), only low levels of α-catenin are detectable in induced PSV2 cells compared to those found in induced P_o-expressing cells.

incorporation in the P_o expressor reaction mixture than in the control. It is likely, therefore, that an upregulation of desmoplakin mRNA transcription, a stabilization of these mRNAs, or both, occurs in the P_o expressor population. Whatever the mechanism, the protein levels of desmoplakin are correspondingly increased in immunoblots of P_o expressors (Fig. 9 *A*, lane *6*) as compared to PSV2 control cells (Fig. 9 *B*, lane *5*). Additional work should elucidate the subcellular basis for the increased mRNA and protein levels of this desmosomal component.

Given the increase in N-cadherin fluorescence at the surface of the expressors, we also looked for a relative change in mRNA levels for N-cadherin in the P_o expressors, as compared with HeLa cell controls. We synthesized degenerate primers against highly homologous putative Ca^{++}-binding domains common to N- and E-cadherin (Hatta et al., 1988) (see Materials and Methods) which were shown to recognize authentic N- and E-cadherin with control template encoding human N- or E-cadherin. As expected from our immunocytochemical data (see above, and Fig. 8, *A–B*), as well as previous work (Ozawa et al., 1989; Herrenknecht et al., 1991; Knudsen, K. A., personal communication) only N-cadherin could be detected when normal Hela cell cDNA was used as a template. These primers were used in PCR reactions containing P_o expressors or HeLa cell cDNA (as above) except isotopic label was omitted. After electrophoresis of the reaction products obtained on completion of cycle 25, gels were incubated in ethidium bromide (Fig. 9 *B*, lanes *1* and *2*), photographed, and processed for DNA blotting using an α^{32}P-labeled human N-cadherin cDNA we isolated as the probe. The ethidium-stained preparations revealed a strong band of the predicted size for human N-cadherin in the reaction mixtures containing cDNA from the P_o expressors (Fig. 9 *B*, lane *1*), but not in reactions from the control cells (Fig. 9 *B*, lane *2*) or when no cDNA template was added (not shown). DNA blots probed with N-cadherin cDNA, autoradiographed and densitometrically scanned revealed at least 10-fold more isotopic label in the P_o expressors (Fig. 9 *B*, lane *4*) than in control cells (Fig. 9 *B*, lane *5*). Molecular cloning of the PCR-amplified DNA from control or P_o expressor reaction mixtures yielded 21 individual colonies, all of which were found by nucleotide sequence analysis to contain plasmids with inserts encoding human N-cadherin exclusively.

Since RT-PCR analysis demonstrated an increase in N-cadherin mRNA in P_o expressors, extracts of PSV2 cells and P_o-expressing cells were subjected to Western blot analysis using monoclonal anti–N-cadherin (Fig. 9 *C*). Corroborating our immunocytochemical data (Fig. 8 *B*), N-cadherin was enriched in P_o expressors (Fig. 9 *C*, P_o). Moreover, there is clearly an increase in N-cadherin protein (Fig. 9 *C*, P_o, [+]) after butyrate treatment increases P_o expression (Fig. 1, *C–E*), when compared to non-butyrate-treated cells (Fig. 9 *C*, P_o, [−]), when there is only a low level of P_o protein in these cells (Fig. 1, *C–E*). In control PSV2 cells, however, N-cadherin was not detected (Fig. 9 *C*, PSV2), either without (−) or with (+) butyrate treatment. The fact that there is an increase in N-cadherin protein levels after an increase in P_o protein (see Fig. 1 *E*), while there is no change in control cells with butyrate treatment, argues strongly that the expression of P_o brings about the increase in N-cadherin found in these cells.

In addition to desmoplakin and N-cadherin, two other proteins, ZO-1 and α-catenin, were detected using immunoblot techniques. Interestingly, ZO-1 protein levels were the same in control and P_o-expressing HeLa cells, with or without butyrate treatment (Fig. 9 *D*), suggesting that the immunocytochemical data (see Fig. 5, *D–E*) reflects a reorganization of existing ZO-1 to cell–cell contact regions. These results also indicate that butyrate treatment specifically stimulates the expression of the P_opECE vector in these cells. Moreover, the ZO-1 immunoblots can serve as an internal standard for the other blots of the cytoskeletal fraction, including desmoplakin (Fig. 9 *A*, lanes *5–6*) and α-catenin (Fig. 9 *E*). Like desmoplakin and N-cadherin, α-catenin is substantially increased in P_o expressors when compared to PSV2 cells (Fig. 9 *E*). These cells therefore appear to show a selective response to P_o-mediated adhesion, the exact nature of which requires further study.

Reorganization of the Keratin Filament Network Occurs in P_o Expressors

A prominent intracellular feature of mature desmosomes are the bundles of intermediate filaments that are found associated with the plaque region (Farquhar and Palade, 1963; Schwarz et al., 1990; Stappenbeck and Green, 1992; Garrod et al., 1993; Stappenbeck et al., 1993). These filaments, composed of organized keratins, are readily observed by transmission electron microscopy, and extend deeply into the cytoplasm on either side of the plasma membrane. Ultrastructurally, we had noted in confluent P_o expressors that shortly after butyrate treatment, plasma membrane thickenings denoting developing desmosomes were clearly apparent (see Fig. 3), but intermediate filament assembly at these structures seemed delayed for several hours. To assess the development of the keratin network, we performed immunohistochemistry on the cultured cells, treating coverslips with antibodies against both desmoplakin (Cowin et al., 1985) and cytokeratin-18 (Ramaekers et al., 1983), known to be expressed in HeLa cells (Moll et al., 1982). In control cell populations (Fig. 10 *A*) keratin filaments frequently appeared elongated and sparsely distributed. In the P_o expressors, however (Fig. 10 *B*), keratin bundles were conspicuous and perinuclear, and in many cases, double labeling with anti-desmoplakin (Fig. 10 *C*) showed that the filament bundles were aligned from one cell to another. In fact, cytokeratin bundles frequently were inserted into the surface desmosomes (Fig. 10 *C*, *arrows*). Slot-blots of total cell lysates from postbutyrate-treated control and P_o expressors probed with keratin antisera revealed virtually equivalent staining intensities in the two populations (not shown). These results indicate that the increase in desmosome formation found in P_o expressors leads to the formation of an intercellular network of keratin filaments from an apparently constant keratin pool.

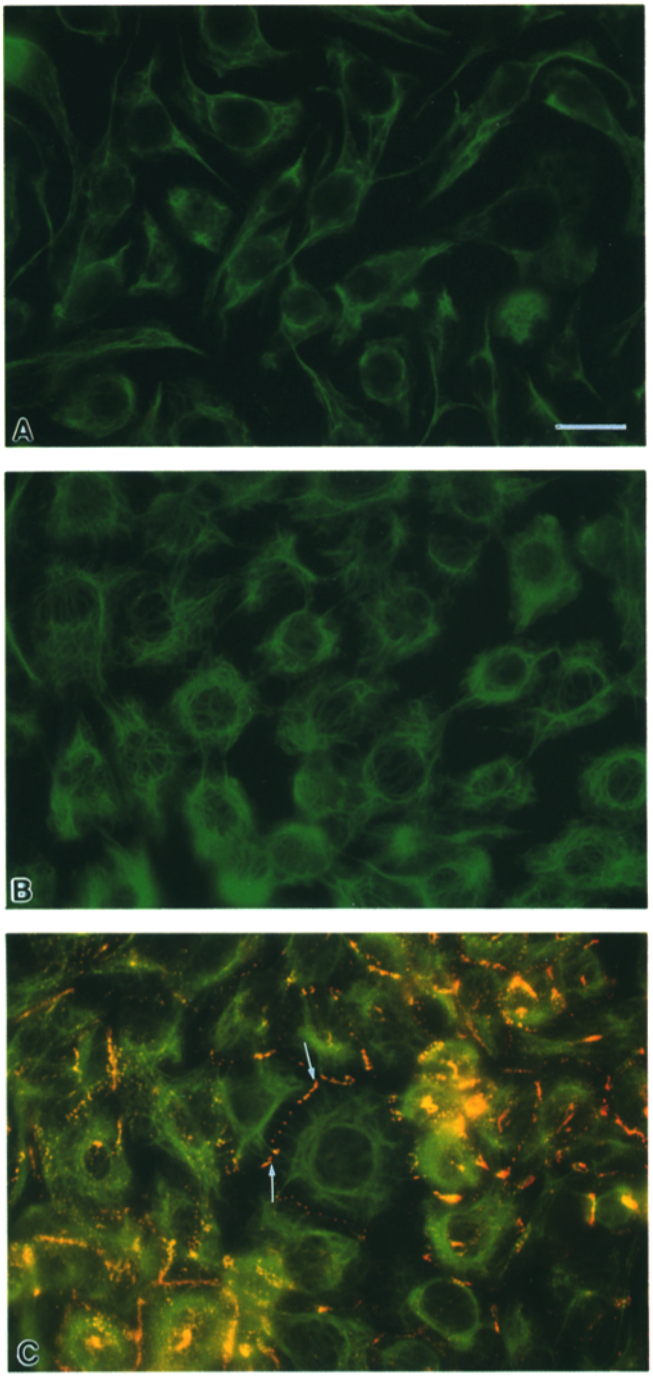

Figure 10. Cytokeratin filaments establish intercellular networks via desmosomal attachments in P_o expressors. (*A*) Cytokeratin 18 immunostaining of control HeLa cells shows elongated keratin filaments. (*B*) Cytokeratin 18 immunolabeling in P_o-expressing HeLa cells reveals perinuclear coalescence of filaments. (*C*) Double immunofluorescence for desmoplakin (*Rh*) and cytokeratin 18 (*FITC*) demonstrates that certain keratin filament bundles are associated with desmoplakin-labeled desmosomes (*arrows*). Bar, 20 μm.

Discussion

It is generally accepted that in forming epithelia, surface interactions between adhesion molecules in the cadherin superfamily are the starting point for the molecular cascade that ultimately leads to the formation of the differentiated phenotype (Geiger and Ayalon, 1992; McNeill et al., 1993; Takeichi, 1991; Wheelock and Jensen, 1992, Watabe et al., 1994). Thereafter, the maintenance of the normal epithelial phenotype requires constant cell–cell contact that is sustained by adhesion molecules expressed on cell surfaces. In many self-adherent epithelial cells the first step in the adhesion process is mediated by uvomorulin (E-cadherin), and it has been proposed that E-cadherin may in many systems exert a hierarchical control over the subsequent formation of junctional elements (Gumbiner et al., 1988; McNeil et al., 1993). HeLa cells however are an unusual epithelial derivative in that although they express cytokeratins (Moll et al., 1982), they do not synthesize detectable levels of E-cadherin, but rather express very low levels of N-cadherin (Herrenknecht et al., 1991; Knudsen, K. A., personal communication, and see Fig. 8). HeLa cells display some epithelial characteristics, but only weakly; for example, they form contact-inhibited epithelial islands at low density and, as shown in Fig. 3, occasional adherens junctions, desmosomes, and tight junctions may be observed. Therefore, the machinery for the synthesis of these complex macromolecular structures ap-

pears undamaged and functional, but normally operates only at a low, sub-basal level that is not optimal for the creation and maintenance of a normal epithelium.

We observed that the expression of P_o has the ability to profoundly affect the adhesive behavior and morphology of normally poorly self-adhesive HeLa cells. Relative to most other IgCAMS, the extracellular domain of P_o is very small, consisting of a 124–amino acid segment that contains within it a single Ig-fold (Lai et al., 1987; Lemke et al., 1988). Homophilic interaction mediated by the mutual binding of this domain across the intermembrane cleft in peripheral nerve myelin yields a broad, continuous and absolutely regular 3–5-nm gap across the extracellular cleft that separates the Schwann cell bilayers (Raine, 1984). A similar size gap has been described by us for the P_o-expressing HeLa cells we used here (see D'Urso et al., 1990). From the morphological and aggregation data, we infer that a similar Ca^{++}-independent homophilic adhesive mechanism mediated by P_o triggers dramatic ultrastructural changes in these transformed cells. Extensive membrane contact and cell–cell aggregation is accompanied by the restricted lateral localization of P_o along zones of cell–cell contact (Fig. 2, Fig. 4, *C* and *D*).

The rapidity of P_o expressor cell aggregation under these conditions compares favorably with the time course of adhesive contact development in monolayers of keratinocytes or MDCK cells upon switching to high Ca^{++} (1–2 mM), cell types in which preexisting components of junctional complexes are believed to assemble to cause epithelialization (Watt et al., 1984; Mattey and Garrod, 1986; Mattey et al., 1990). However, in cells such as keratinocytes, mature desmosomes are assembled within a very short time after cell–cell contact is established (Hennings and Holbrook, 1983; Watt et al., 1984) because all polypeptide components are apparently already present in sufficient quantity to yield the rapid assembly of desmosomes under the right conditions. Other studies have shown that the initial events in the process of reassembly of a previously formed epithelial monolayer do not require either the induction of relevant genes or de novo protein synthesis of junctional components (Pasdar and Nelson, 1988*a*,*b*; Hennings and Holbrook, 1983;), although long term development relies heavily on new protein synthesis (Mattey et al., 1990). These studies used epithelial cells grown under culture conditions either of low Ca^{++} or low cell density, in which preexisting intracellular pools of junctional components are present that can be readily mobilized and assembled once cell–cell adhesion has been initiated. In contrast, the generation of the epithelial phenotype in the HeLa cell line used in our studies fundamentally differs in that initial close membrane contact is brought about by the expression of a "foreign" homophilic adhesion molecule by these cells.

Our most striking observation was that by obligating HeLa cells to adhere to one another along extensive areas through the surface expression of P_o, the formation of certain junctional complexes characteristic of normal epithelial tissues was dramatically enhanced. P_o-P_o interaction in this context clearly acts adhesively before, or in conjunction with, what has been traditionally viewed as the *sine qua non* for epithelialization; i.e., the cadherin-catenin adhesion system (Watabe et al., 1994). Our data reveal that newly formed linear arrays of desmosomes, whose major integral membrane components (desmocollin and desmoglein) are cadherins (Goodwin et al., 1990; Holton et al., 1990; Koch et al., 1990; Mechanic et al., 1991), arise progressively within an extensive, previously formed island of P_o adhesion (Fig. 6), analogous to the "zippering" spread of stable contacts that have been observed between epithelial cells during early stages of cell–cell adhesion (McNeill et al., 1993). Since P_o adhesion allows membranes to engage at a minimal distance (3–5 nm), and the mature desmosome separates bilayers by ~30 nm, it may be expected that P_o-mediated adhesion cannot continue to operate where mature desmosomes "embedded" in the P_o adhesion zone are present.

In addition to desmosome formation, P_o induced cell–cell adhesion also dramatically enhances the organization of tight junctional and adherens junction associated proteins at the lateral contact sites. Although there is clearly some low level expression of adhesion molecules in these cells (e.g., Fig. 7, *A* and *C*), normally their contribution to cell–cell adhesion in this carcinoma must be minimal. The expression of a strong, functional, adhesion molecule such as P_o in HeLa cells therefore seems to convey the additional adhesivity necessary for the formation of junctions characteristic of epithelial tissues. Similarly, when the adhesive properties of S180 mouse sarcoma cells were enhanced by expression of L-CAM, a cadherin, or when these cells were agglutinated with lectins, functional gap junctions formation was increased (Mege et al., 1988), a result of the appropriate phosphorylation of connexin 43 (Musil et al., 1990). However, when the neural cell adhesion molecule (NCAM), a member of the immunoglobulin gene superfamily, was expressed in S180 cells, functional gap junctions did not develop, even though NCAM has previously been shown to have certain adhesive properties (Edelman et al., 1987; Williams and Barclay, 1988). "Strong" cell–cell adhesion, such as that brought about by cadherins (Shapiro et al., 1995) or the immunoglobulin P_o, may therefore be necessary for the marked effects on the cytoarchitecture and physiology of the cells involved. We should emphasize that we did not attempt to test for functionality of any of the junctional elements we examined.

The subcellular mechanisms by which P_o brings about dramatic changes in HeLa cells have not been directly examined here, but it can be adduced from these studies, and from what is known about P_o function in Schwann cells, that this molecule acts initially to bring adjacent plasma membranes and their integral membrane proteins into close apposition, allowing the formation of stabilizing junctional complexes and perhaps eliciting second messenger pathways. In this model, P_o acts solely to overcome the "functional repulsion" that seems to exist between normal HeLa cells. Once initiated, cell–cell adhesion is undoubtedly reinforced by adhesion-based structures, the desmosomes and adherens junctions which use cadherins as major integral membrane adhesion molecules. Although N-cadherin (Figs. 8 and 9) is not usually recognized as a key contributor to epithelial cell–cell adhesion, it may play a critical role in the morphological changes seen in P_o-expressing HeLa cells. When PC12 cells, which normally express N-cadherin, are placed in contact with N-cadherin–expressing NIH3T3 cells, they differentiate, assuming a

neuronal morphology (Doherty et al., 1991). This transition can be mimicked by direct activation of second messenger systems, suggesting that the homophilic association of N-cadherin is one activator of an intracellular signaling pathway. The cytoplasmic domain of N-cadherin is known to bind to catenins (Ozawa and Kemler, 1992; Hirano et al., 1992), cytoskeletal proteins that may be involved in the second messenger cascade that may be activated in these cells after P_0 initially brings adjacent plasma membranes into close apposition. Speculatively, no matter how the adhesion cascade is initially triggered, induction of an intracellular messenger system that is common to all epithelia, and that controls the implementation of the adhesion program may rapidly follow.

While recent results demonstrate that the cytoplasmic domain of P_0 is necessary for aggregation of P_0-transfected cells in suspension (Wong and Filbin, 1994), suggestive of interactions between P_0 and the cytoskeleton, the cytoplasmic domain of P_0 has no known intracellular signaling properties. In Schwann cells, P_0 is absolutely and precisely targeted after synthesis to the forming compact myelin plasma membrane domain, effectively removing it from cell membrane circulation. Furthermore, the intact cytoplasmic segment of P_0 may be nonessential for triggering of the adhesion response in HeLa cells, since in preliminary experiments we have observed that an engineered P_0 extracellular domain that is missing the cytoplasmic segment but is anchored to the plasma membrane via a glycosylphosphotidyl inositol moiety, can mediate similar changes in HeLa cell morphology.

In summary, our results support a model in which P_0, a strong membrane adhesion molecule, by maintaining close membrane contact, allows the development of stabilizing adhesive junctions and the interaction of molecules possibly involved in second messenger signaling. The dramatic reorganization of tight junction–associated proteins, desmosomal proteins, and adherens junction proteins leads these transformed cells to display a differentiated, classic epithelial phenotype. Perhaps most important, the regeneration of this phenotype is correlated, at least in this cell type, with the engagement of the cadherin Ca^{++}-dependent adhesion system and the subcortical components through which they are able to transduce changes in cell morphology. P_0-mediated compaction of peripheral nerve myelin may similarly affect the expression or localization of native myelin proteins (Doyle and Colman, 1993) including the recently described cadherin/catenin system in myelinating Schwann cells (Fannon et al., 1995). In HeLa cells, P_0 clearly initiates an adhesion cascade, but the sequence of events that follow have not been clarified as yet. One model, alluded to above, is that the close membrane apposition "enforced" by P_0 stabilizes the interaction of extremely low levels of cell surface cadherins (N-cadherin, desmocollin, and desmoglein) that would otherwise be insufficient to trigger epithelioid development of the monolayer. In this model, an increase in junctional proteins at cell surfaces ensues and common intracellular pathways are used to yield epithelialization.

On the other hand, P_0 may possibly have as yet unrecognized intracellular messenger properties itself that directly activate common adhesive programs, bypassing the cadherin adhesion cascade. P_0 therefore may simultaneously compact cell membranes and trigger the subsequent steps leading to a general enhancement of the epithelial program. In this scenario, the upregulation of junctional markers we observed at the cell surface would then be an indirect consequence of P_0 activation.

The authors thank Eric Hubel and Lazar Fidler for preparation of the figures. This is manuscript number 183 from The Brookdale Center for Molecular Biology.

This work was supported by grants to D. R. Colman (NINDS NS 20147) and to P. Cowin (GM 47429) from the National Institutes of Health. D. D'Urso is an Alexander von Humboldt Fellow on leave from the Laboratory of Pathophysiology, Istituto Superiore di Sanita (Rome, Italy).

Received for publication 7 December 1994 and in revised form 20 June 1995.

References

Albelda, S. M., and C. A. Buck. 1990. Integrins and other cell adhesion molecules. *FASEB (Fed. Am. Soc. Exp. Biol.) J.* 4:2868–2880.

Allinquant, B., S. M. Staugaitis, D. D'Urso, and D. R. Colman. 1991. The ectopic expression of myelin basic protein isoforms in *Shiverer* oligodendrocytes: implications for myelinogenesis. *J. Cell Biol.* 113:393–403.

Anderson, J. M., B. R. Stevenson, L. A. Jesaitis, D. A. Goodenough, and M. S. Mooseker. 1987. Characterization of ZO-1, a protein component of the tight junction from mouse liver and Madin-Darby canine kidney cells. *J. Cell Biol.* 106:1141–1149.

Birchmeier, W., J. Beherens, K. Weidner, U. Frixen, and J. Schipper. 1991. Dominant and recessive genes involved in tumor cell invasion. *Curr. Opin. Cell Biol.* 3:832–840.

Boller, K., D. Vestweber, and R. Kemler. 1985. Cell adhesion molecule uvomorulin is localized in the intermediate junctions of adult intestinal epithelial cells. *J. Cell Biol.* 100:327–332.

Brackenbury, R., J. P. Thiery, U. Rutishauser, and G. Edelman. 1977. Adhesion among neural cells of the chick embryo. I. An immunological assay for molecules involved in cell-cell binding. *J. Biol. Chem.* 252:6835–6840.

Chomczynski, P., and N. Sacchi. 1987. Single-step method of RNA isolation by acid guanidinium thiocyanate-phenol-chloroform extraction. *Anal. Biochem.* 162:156–159.

Citi, S., H. Sabanay, R. Jakes, B. Geiger, and J. Kendrick-Jones. 1988. Cingulin, a new peripheral component of tight junctions. *Nature (Lond.).* 333:272–276.

Citi, S., H. Sabanay, R. Jakes, J. Kendrik-Jones, and B. Geiger. 1989. Cingulin: characterization and localization. *J. Cell Sci.* 93:107–122.

Cowin, P., and D. R. Garrod. 1983. Antibodies to epithelial desmosomes show wide tissue and species cross-reactivity. *Nature (Lond.).* 302:148–150.

Cowin, P., and A. M. C. Brown. 1993. Components of intercellular adhesive junctions and their roles in morphogenesis. *In* Molecular Basis of Morphogenesis. Wiley-Liss, Inc., New York. pp 49–67.

Cowin, P., H. Kapprell, and W. W. Franke. 1985. The complement of desmosomal plaque proteins in different cell types. *J. Cell Biol.* 101:1442–1454.

Damsky, C. H., J. Richa, D. Solter, K. Knudsen, and C. A. Buck. 1983. Identification and purification of a cell surface glycoprotein mediating intercellular adhesion in embryonic and adult tissue. *Cell.* 34:455–466.

Devereux, J., P. Haeberli, and O. Smithies. 1984. A comprehensive set of sequence analysis programs for the VAX. *Nucleic Acids Res.* 12:387–395.

Doherty, P., S. V. Ashton, S. E. Moore, and F. S. Walsh. 1991. Morphoregulatory activities of NCAM and N-cadherin can be accounted for by G protein-dependent activation of L- and N-type neuronal Ca^{2+} channels. *Cell.* 67: 21–33.

Doyle, J. P., and D. R. Colman. 1993. Glial-neuron interaction and the regulation of myelin formation. *Curr. Opin. Cell Biol.* 5:779–785.

D'Urso, D., P. J. Brophy, S. M. Staugaitis, C. S. Gillespie, A. B. Frey, J. G. Stempak, and D. R. Colman. 1990. Protein zero of peripheral nerve myelin: biosynthesis, membrane insertion, and evidence for homotypic interaction. *Neuron.* 4:449–460.

Edelman, G. M., B. A. Murray, R. M. Mege, B. A. Cunningham, and W. A. Gallin. 1987. Cellular expression of liver and neural cell adhesion molecules after transfection with their cDNAs results in specific cell-cell binding. *Proc. Natl. Acad. Sci. USA.* 84:8502–8506.

Ellis, L., E. Clauser, D. O. Morgan, M. Edery, R. A. Roth, and W. J. Rutter. 1986. Replacement of insulin receptor tyrosine residues 1162 and 1163 compromises insulin-stimulated kinase activity and uptake of 2-deoxyglucose. *Cell.* 45:721–732.

Fannon, A. M., D. L. Sherman, G. Ilyana-Gragerova, P. J. Brophy, V. L. Friedrich, Jr., and D. R. Colman. 1995. Novel E-cadherin-mediated adhesion in peripheral nerve: Schwann cell architecture is stabilized by autotypic adherens junctions. *J. Cell Biol.* 129:189–202.

Farquhar, M. G., and G. E. Palade. 1963. Junctional complexes in various epithelia. *J. Cell Biol.* 17:375–412.

Feinberg, A. P., and B. Vogelstein. 1983. A technique for radiolabeling DNA restriction endonuclease fragments to high specific activity. *Anal. Biochem.* 132:6–13.

Filbin, M., F. Walsh, B. Trapp, J. Pizzey, and G. Tennekoon. 1990. Role of myelin P_0 protein as a homophilic adhesion molecule. *Nature (Lond.).* 344:871–872.

Franke, W. W., D. L. Schiller, R. Moll, S. Winter, E. Schmid, I. Engelbrecht, H. Denk, R. Krepler, and B. Platzer. 1981. Diversity of cytokeratins: differentiation specific expression of cytokeratin polypeptides in epithelial cells and tissues. *J. Mol. Biol.* 153:933–959.

Frixen, U. H., J. Behrens, M. Sachs, G. Eberle, B. Voss, A. Warda, D. Lochner, and W. Birchmeier. 1991. E-cadherin-mediated cell-cell adhesion prevents invasiveness of human carcinoma cells. *J. Cell Biol.* 113:173–185.

Garrod, D. R. 1993. Desmosomes and hemidesmosomes. *Curr. Opin. Cell Biol.* 5:30–40.

Geiger, B. 1979. A 130K protein from chicken gizzard: its localization at the termini of microfilament bundles in cultured chicken cells. *Cell.* 18:193–205.

Geiger, B., and O. Ayalon. 1992. Cadherins. *Annu. Rev. Cell Biol.* 8:307–332.

Geiger, B., T. Volk, T. Volberg, and R. Bendori. 1987. Molecular interactions in adherens-type contacts. *J. Cell Sci. Suppl.* 8:251–272.

Goneharova, E. J., Z. Kam, and B. Geiger. 1992. The involvement of adherens junction components in myofibrillogenesis in cultured cardiac myocytes. *Development.* 114:173–183.

Goodwin, L., J. E. Hill, K. Raynor, L. Raszi, M. Marabe, and P. Cowin. 1990. Desmoglein shows extensive homology to the cadherin family of cell adhesion molecules. *Biochem. Biophys. Res. Commun.* 173:1224–1230.

Gorman, C., B. Howard, and R. Reeves. 1983. Expression of recombinant plasmids in mammalian cells is enhanced by sodium butyrate. *Nucleic Acids Res.* 11:7631–7648.

Green, K. J., D. A. D. Parry, P. M. Steinert, M. L. A. Virata, R. M. Wagner, B. D. Angst, and L. A. Nilles. 1990. Structure of the human desmoplakins. Implications for function in the desmosomal plaque. *J. Biol. Chem.* 265:2603–2612.

Gumbiner, B. M. 1993. Proteins associated with the cytoplasmic surface of adhesion molecules. *Neuron.* 11:551–564.

Gumbiner, B., B. Stevenson, and A. Grimaldi. 1988. The role of the cell adhesion molecule uvomorulin in the formation and maintenance of the epithelial junctional complex. *J. Cell Biol.* 107:1575–1587.

Hatta, K., A. Nose, A. Nagafuchi, and M. Takeichi. 1988. Cloning and expression of cDNA encoding a neural calcium-dependent cell adhesion molecule: its identity in the cadherin gene family. *J. Cell Biol.* 106:873–881.

Hennings, H., and K. A. Holbrook. 1983. Calcium regulation of cell-cell contact and differentiation of epidermal cells in culture. *Exp. Cell Res.* 143:127–142.

Herrenknecht, K., M. Ozawa, C. Eckerson, F. Lottspeich, M. Lenter, and R. Kemler. 1991. The uvomorulin-anchorage protein α-catenin is a vinculin homologue. *Proc. Natl. Acad. Sci. USA.* 88:9156–9160.

Hinck, L., I. S. Näthke, J. Papkoff, and W. J. Nelson. 1994. Dynamics of cadherin/catenin complex formation: novel protein interactions and pathways of complex assembly. *J. Cell Biol.* 125:1327–1340.

Hirano, S., N. Kimoto, Y. Shimoyama, S. Hirohashi, and M. Takeichi. 1992. Identification of a neural α-catenin as a key regulator of cadherin function and multicellular organization. *Cell.* 70:293–301.

Hirano, S., A. Nose, K. Hatta, A. Kawakami, and M. Takeichi. 1987. Calcium-dependent cell-cell adhesion molecules (cadherins): subclass specificities and possible involvement of actin bundles. *J. Cell Biol.* 105:2501–2510.

Holton, J. L., T. P. Kenny, P. K. Legan, J. E. Collins, J. N. Keen, R. Sharma, and D. R. Garrod. 1990. Desmosomal glycoproteins 2 and 3 (desmocollins) show N-terminal similarity to calcium-dependent cell-cell adhesion molecules. *J. Cell Sci.* 97:239–246.

Howarth, A. G., M. R. Hughes, and B. R. Stevenson. 1992. Detection of the tight junction-associated protein ZO-1 in astrocytes and other nonepithelial cell types. *Am. J. Physiol.* 262:C461–C469.

Howarth A. G., K. L. Singer, and B. R. Stevenson. 1994. Analysis of the distribution and phosphorylation state of ZO-1 in MDCK and nonepithelial cells. *J. Membr. Biol.* 137:261–270.

Hynes, R. O. 1992. Integrins: versatility, modulation, and signalling in cell adhesion. *Cell.* 69:11–25.

Itoh, M., A. Nagafuchi, S. Yonemura, T. Kitani-Yasuda, S. Tsukita, and S. Tsukita. 1993. The 220-kD protein colocalizing with cadherins in nonepithelial cells is identical to ZO-1, a tight junction–associated protein in epithelial cells: cDNA cloning and immunoelectron microscopy. *J. Cell Biol.* 121:491–502.

Koch, P. J., M. J. Walsh, M. Schmelz, M. D. Goldschmidt, R. Zimbelmann, and W. W. Franke. 1990. Identification of desmoglein, a constitutive desmosomal glycoprotein, as a member of the cadherin family of cell adhesion molecules. *Eur. J. Cell Biol.* 53:1–12.

Lai, C., M. A. Brow, K. Nave, A. B. Noronha, R. H. Quarles, F. E. Bloom, R. J. Milner, and J. G. Sutcliffe. 1987. Two forms of 1B236/myelin-associated glycoprotein, a cell adhesion molecule for postnatal neural development, are produced by alternative splicing. *Proc. Natl. Acad. Sci. USA.* 84:4337–4341.

Lemke, G., and R. Axel. 1985. Isolation and sequence of a cDNA encoding the major structural protein of peripheral myelin. *Cell.* 40:501–508.

Lemke, G., E. Lamar, and J. Patterson. 1988. Isolation and analysis of the gene encoding peripheral myelin protein zero. *Neuron.* 1:73–83.

Mattey, D. L., and D. R. Garrod. 1986. Calcium-induced desmosome formation in cultured kidney epithelial cells. *J. Cell Sci.* 85:95–111.

Mattey, D. L., G. Burdge, and D. R. Garrod. 1990. Development of desmosomal adhesion between MDCK cells following calcium switching. *J. Cell Sci.* 97:689–704.

McNeill, H., T. A. Ryan, S. J. Smith, and W. J. Nelson. 1993. Spatial and temporal dissection of immediate and early events following cadherin-mediated epithelial cell adhesion. *J. Cell Biol.* 120:1217–1226.

Mechanic, S., K. Raynor, J. E. Hill, and P. Cowin. 1991. Desmocollins form a distinct subset of the cadherin family of cell adhesion molecules. *Proc. Natl. Acad. Sci. USA.* 88:4476–4480.

Mege, R.-M., F. Matsuzaki, W. J. Gallin, J. Goldberg, B. A. Cunningham, and G. M. Edelman. 1988. Construction of epithelioid sheets by transfection of mouse sarcoma cells with cDNAs for chicken cell adhesion molecules. *Proc. Natl. Acad. Sci. USA.* 85:7274–7278.

Moll, R., W. W. Franke, and D. L. Schiller. 1982. The catalog of human cytokeratins: patterns of expression in normal epithelia, tumors, and cultured cells. *Cell.* 31:11–24.

Musil, L. S., B. A. Cunningham, G. M. Edelman, and D. A. Goodenough. 1990. Differential phosphorylation of the gap junction protein connexin43 in junctional communication-competent and -deficient cell lines. *J. Cell Biol.* 111: 2977–2988.

Nagafuchi, A., S. Ishihara, and S. Tsukita. 1994. The roles of catenins in the cadherin-mediated cell adhesion: functional analysis of E-cadherin-α catenin fusion molecules. *J. Cell Biol.* 127:235–245.

Nagafuchi, A., Y. Shirayoshi, K. Okazaki, K. Yasuda, and M. Takeichi. 1987. Transformation of cell adhesion properties by exogenously introduced E-cadherin cDNA. *Nature (Lond.).* 329:341–343.

Nagafuchi, A., M. Takeichi, and S. Tsukita. 1991. The 102 kD cadherin-associated protein: similarity to vinculin and posttranscriptional regulation of expression. *Cell.* 65:849–857.

Näthke, I. S., L. Hinck, J. R. Swedlow, J. Papkoff, and W. J. Nelson. 1994. Defining interactions and distributions of cadherin and catenin complexes in polarized epithelial cells. *J. Cell Biol.* 125:1341–1352.

Navarro, P., M. Gómez, A. Pizzaro, C. Gamallo, M. Quintanilla, and A. Cano. 1991. A role for the E-cadherin cell-cell adhesion molecule during tumor progression of mouse epidermal carcinogenesis. *J. Cell Biol.* 115:517–533.

Ozawa, M., H. Baribault, and R. Kemler. 1989. The cytoplasmic domain of the cell adhesion molecule uvomorulin associates with three independent proteins structurally related in different species. *EMBO (Eur. Mol. Biol. Organ.) J.* 8:1711–1717.

Ozawa, M., and R. Kemler. 1992. Molecular organization of the uvomorulin-catenin complex. *J. Cell Biol.* 116:989–996.

Pasdar, M., K. Krzeminski, and W. J. Nelson. 1991. Regulation of desmosome assembly in MDCK epithelial cells: coordination of membrane core and cytoplasmic plaque domain assembly at the plasma membrane. *J. Cell Biol.* 113:645–655.

Pasdar, M., and W. J. Nelson. 1988*a*. Kinetics of desmosome assembly in Madin-Darby canine kidney epithelial cells: temporal and spatial regulation of desmoplakin organization and stabilization upon cell–cell contact. I. Biochemical analysis. *J. Cell Biol.* 106:677–685.

Pasdar, M., and W. J. Nelson. 1988*b*. Kinetics of desmosome assembly in Madin-Darby canine kidney epithelial cells: temporal and spatial regulation of desmoplakin organization and stabilization upon cell–cell contact. II. Morphological analysis. *J. Cell Biol.* 106:687–695.

Ramaekers, F. C. S., A. Huysmans, O. Moesker, A. Kant, P. Jap, C. Herman, and P. Vooijs. 1983. Monoclonal antibody to keratin filaments specific for glandular epithelia and their tumours: use in surgical pathology. *Lab Invest.* 49:353–361.

Raine, C. S. 1984. Morphology of myelin and myelination. *In* Myelin. P. Morell, editor. Plenum Publishing Corp., New York. pp. 1–50.

Reid, R. A., and J. J. Hemperly. 1990. Human N-cadherin:nucleotide and deduced amino acid sequence. *Nucleic Acids Res.* 18:5896.

Rodriguez-Boulan, E., and W. J. Nelson. 1989. Morphogenesis of the polarized epithelial cell phenotype. *Science (Wash. DC).* 245:718–725.

Schmelz, M., R. Duden, P. Cowin, and W. W. Franke. 1986. A constitutive transmembrane glycoprotein of Mr 165,000 (desmoglein) in epidermal and non-epidermal desmosomes. I. Biochemical identification of the polypeptide. *Eur. J. Cell Biol.* 42:177–83.

Schneider-Schaulies, J., A. von Brunn, and M. Schachner. 1990. Recombinant peripheral myelin protein P_0 confers both adhesion and neurite outgrowth-promoting properties. *J. Neurosci. Res.* 27:286–297.

Schwarz, M. A., K. Owaribe, J. Kartenbeck, and W. W. Franke. 1990. Desmosomes and hemidesmosomes: constitutive molecular components. *Annu. Rev. Cell Biol.* 6:461–491.

Shapiro, L., A. M. Fannon, P. D. Kwong, A. Thompson, M. S. Lehmann, G. Grübel, J.-F. Legrand, J. Als-Nielson, D. R. Colman, and W. A. Hendrickson. 1995. Structural basis of cell-cell adhesion by cadherins. *Nature (Lond.).* 374:327–337.

Southern, P. J., and P. Berg. 1982. Transformation of mammalian cells to antibiotic resistance with a bacterial gene under control of the SV40 early region promoter. *J. Mol. Appl. Gen.* 1:327–341.

Stappenbeck, T. S., and K. J. Green. 1992. The desmoplakin carboxyl terminus coaligns with and specifically disrupts intermediate filament networks when expressed in cultured cells. *J. Cell Biol.* 116:1197–1209.

Stappenbeck, T. S., E. A. Bornslaeger, C. M. Corcoran, H. H. Luu, M. L. A. Vi-

rata, and K. J. Green. 1993. Functional analysis of desmoplakin domains: specification of the interaction with keratin vs vimentin intermediate filament network. *J. Cell Biol.* 123:691–705.

Staugaitis, S. M., P. R. Smith, and D. R. Colman. 1990. Expression of myelin basic protein isoforms in nonglial cells. *J. Cell Biol.* 110:1719–1727.

Stevenson, B. R., J. D. Siliciano, M. S. Mooseker, and D. A. Goodenough. 1986. Identification of ZO-1: a high molecular weight polypeptide associated with the tight junction (zonula occludens) in a variety of epithelia. *J. Cell Biol.* 103:755–766.

Takeichi, M. 1991. Cadherin cell adhesion receptors as a morphogenetic regulator. *Science (Wash. DC).* 25:1451–1455.

Takeichi, M. 1993. Cadherins in cancer: implications for invasion and metastasis. *Curr. Opin. Cell Biol.* 5:806–811.

Tokunaga, K., Y. Nakamura, K. Sakata, K. Fujimori, M. Ohkubo, K. Sawada, and S. Sakiyama. 1987. Enhanced expression of a glyceraldehyde-3-phosphate dehydrogenase gene in human lung cancers. *Cancer Res.* 47:5616–5619.

Tsukita, S., S. Tsukita, A. Nagafuchi, and S. Yonemura. 1992. Molecular linkage between cadherins and actin filaments in cell-cell adherens junctions. *Curr. Opin. Cell Biol.* 4:834–839.

Vleminckx, K., L. Vakaet, Jr, M. Mareel, W. Fiers, and F. Van Roy. 1991. Genetic manipulation of E-cadherin expression by epithelial tumor cells reveals an invasion suppressor role. *Cell.* 66:107–119.

Volk, T., and B. Geiger. 1986*a*. A-CAM: a 135-kD receptor of intercellular adherens junctions. I. Immunoelectron microscopic localization and biochemical studies. *J. Cell Biol.* 103:1441–1450.

Volk, T., and B. Geiger. 1986*b*. A-CAM: a 135-kD receptor of intercellular adherens junctions. II. Antibody-mediated modulation of junction formation. *J. Cell Biol.* 103:1451–1464.

Volk, T., T. Volberg, I. Sabanay, and B. Geiger. 1990. Cleavage of A-CAM by endogenous proteinases in cultured lens cells and in developing chick embryos. *Dev. Biol.* 139:314–326.

Watabe, M., A. Nagafuchi, S. Tsukita, and M. Takeichi. 1994. Induction of polarized cell–cell association and retardation of growth by activation of the E-cadherin-catenin adhesion system in a dispersed carcinoma line. *J. Cell Biol.* 127:247–256.

Watt, F. M., D. L. Mattey, and D. R. Garrod. 1984. Calcium-induced reorganization of desmosomal components in cultured human keratinocytes. *J. Cell Biol.* 99:2211–2215.

Wheelock, M. J., and P. J. Jensen. 1992. Regulation of keratinocyte intercellular junction organization and epidermal morphogenesis by E-cadherin. *J. Cell Biol.* 117:415–425.

Williams, A. F., and A. N. Barclay. 1988. The immunoglobulin superfamily: domains for cell surface recognition. *Annu. Rev. Immunol.* 6:381–405.

Willott, E., M. S. Balda, M. Heintzelman, B. Jameson, and J. M. Anderson. 1992. Localization and differential expression of two isoforms of the tight junction protein ZO-1. *Am. J. Physiol.* 262:C1119–C1124.

Wollner, D. A., K. A. Krzeminski, and W. J. Nelson. 1992. Remodeling the cell surface distribution of membrane proteins during the development of epithelial cell polarity. *J. Cell Biol.* 116:889–899.

Wong, M., and M. T. Filbin. 1994. The cytoplasmic domain of the myelin P_o protein influences the adhesive interactions of its extracellular domain. *J. Cell Biol.* 126:1089–1097.